



A dynamical systems model of unorganized segregation in two neighborhoods

D. J. Haw & S. J. Hogan

To cite this article: D. J. Haw & S. J. Hogan (2020): A dynamical systems model of unorganized segregation in two neighborhoods, *The Journal of Mathematical Sociology*, DOI: [10.1080/0022250X.2019.1695608](https://doi.org/10.1080/0022250X.2019.1695608)

To link to this article: <https://doi.org/10.1080/0022250X.2019.1695608>



Published online: 17 Jan 2020.



Submit your article to this journal



Article views: 23



View related articles



View Crossmark data



A dynamical systems model of unorganized segregation in two neighborhoods

D. J. Haw^a and S. J. Hogan ^b

^aSchool of Public Health, Imperial College London, London, UK; ^bDepartment of Engineering Mathematics, University of Bristol, Bristol, UK

ABSTRACT

We present a complete analysis of the Schelling dynamical system of two connected neighborhoods, with or without population reservoirs, for different types of linear and nonlinear tolerance schedules. We show that stable integration is only possible when the minority is small and combined tolerance is large. Unlike the case of the single neighborhood, limiting one population does not necessarily produce stable integration and may destroy it. We conclude that a growing minority can only remain integrated if the majority increases its own tolerance. Our results show that an integrated single neighborhood may not remain so when a connecting neighborhood is created.

ARTICLE HISTORY

Received 29 July 2019

Revised 18 November 2019

Accepted 18 November 2019

KEYWORDS

Unorganized Segregation;
Schelling; Bounded
Neighbourhood Model;
Dynamical System

1. Introduction

Segregation in society takes on many forms, occurring not only in ethnicity or religion, but also gender, for example amongst toddlers (Moller & Serbin, 1996) and in professional hierarchies (Clifton et al., 2019). Segregation is seen as so divisive that some have argued it “puts the whole idea of a peaceful society with its constitutional and civic liberties at risk.” (cited in Pancs & Vriend, 2007, p. 4), with €1.1B allocated to integration efforts by the Netherlands in 2003 (cited in Pancs & Vriend, 2007, p. 4).

Schelling’s seminal work on segregation (Schelling, 1969, 1971) is well known for its use of agent-based modeling to explain unorganized segregation. These papers have been cited thousands of times and inspired innumerable other works. They are also the subject of controversy in terms of precedence (Hegselmann, 2017) and applicability (Fossett, 2006).

What appears less well known is that, in the same two papers, Schelling introduced another model, the bounded neighborhood model (BNM) of unorganized segregation. In Schelling’s BNM, a neighborhood is like a district within a city. Within the neighborhood, every member is concerned about the overall population mixture, not with any particular configuration. A member moves out if they are not happy with the population mixture.

Suppose that the population of a single neighborhood is divided into two types and let $X(t), Y(t) \geq 0$ represent the respective population sizes, as a function of time t . In this neighborhood, tolerance limits are allocated to a given population type via a tolerance schedule, as follows². The X -population tolerance schedule $R_X(X)$ describes the minimum ratio Y/X required in order for

CONTACT S. J. Hogan s.j.hogan@bristol.ac.uk Department of Engineering Mathematics, University of Bristol, Bristol BS8 1UB, UK

¹The modern usage would be self-organized.

²Tolerance is a measure of how members of one population remain in an area where there is another population present. In contrast, homophily (or self-segregation) (Clifton et al., 2019) is a measure of how much one population seeks out members of the same population.

all of the X -population to remain in that neighborhood. A similar function $R_Y(Y)$ denotes the tolerance schedule of the Y -population.

Schelling (Schelling, 1969, 1971) made the following assumptions:

- S1. The neighborhood is preferred over other locations: populations of either type will enter/remain/leave unless tolerance conditions are violated.
- S2. The tolerance schedule is neighborhood-specific.
- S3. Each member of the population is aware of the ratio of population types within the neighborhood at the moment the decision is made to enter/remain/leave (perfect information).
- S4. There is no lower bound on tolerance: no population insists on the presence of the other type.
- S5. Tolerance schedules are **monotone decreasing**, the more tolerant population members are the first to enter and the last to leave.

We gave the first dynamical systems formulation of Schelling's BNM in (Haw & Hogan, 2018).

This work studies the continuous movement of two populations in and out of a single neighborhood.

We presented the first complete quantitative analysis of the model for *linear* tolerance schedules.

A fully predictive model was derived and each term within the model was associated with a social meaning. Schelling's qualitative results were recovered and generalized.

For the case of unlimited population movement, we derived exact formulae for regions in parameter space where stable integrated populations can occur and showed how *neighborhood tipping* can be explained in terms of basins of attraction. When population numbers are limited, we derived exact criteria for the occurrence of integrated populations.

A natural extension of (Haw & Hogan, 2018) is to consider multiple neighborhoods, constructing sets of differential equations that describe the flow of population within and between these neighborhoods. In this paper, we focus on the case of two populations $X(t), Y(t)$ moving within and between two neighborhoods. Our work is related to the “two-room model” of segregation studied in (Shin & Sayama, 2014; Shin, Sayama, & Choi, 2016). Our approach differs in that we work in continuous time, whereas they work in discrete time.

We structure the paper as follows. In Section 2, we consider the situation in which both populations are contained solely within the two neighborhoods, so that any population leaving one neighborhood must necessarily relocate to the other. We consider linear tolerance schedules, examining cases when the tolerance schedules are the same or different in both neighborhoods.

We examine the case when one population has its numbers limited in one area (Section 3), and look at how nonlinearity in the tolerance schedules can change outcomes (Section 4).

We discuss our results in Section 5. We consider the situation where there are reservoirs of both populations, outside the two neighborhoods. Whilst the total population of each type in the whole system is conserved, populations can enter or exit either neighborhood without recourse to the other neighborhood. We also examine similarities between the one- and the two-neighborhood problems and consider what happens when a second neighborhood is added to the single neighborhood problem.

Our conclusions are presented in Section 6.

2. Linear tolerance schedules

Recall that for one neighborhood with two populations X, Y , where population members can come and go depending on their tolerance, the dynamical system derived in (Haw & Hogan, 2018, Equation (27)) is given by

$$\begin{aligned} \frac{dX}{dt} &= X[XR_X(X) - Y], \\ \frac{dY}{dt} &= Y[YR_Y(Y) - X] \end{aligned} \tag{1}$$

for general tolerance schedules $R_X(X), R_Y(Y)$. This model satisfies the constraints on the X -population that $\frac{dX}{dt} \geq 0$ when $R_X(X) \geq \frac{Y}{X}$: in other words, the X -population grows (decays) when the tolerance schedule $R_X(X)$ exceeds (falls short of) Y/X and that $\frac{dX}{dt} = 0$ when $X = 0$. The model satisfies similar constraints on the Y -population. Schelling's initial example of a tolerance schedule is linear, as shown in Figure 1. We set

$$\begin{aligned} R_X(X) &= a(1 - X), \\ R_Y(Y) &= b(1 - kY), \end{aligned} \quad (2)$$

where we scale the size of the X -population to 1 and the minority Y -population to $1/k$, where $k \geq 1$. With our scalings, the most tolerant member of the X -population can abide a RPCS-A_1704844 ratio of $a > 0$ and the least tolerant member of the X -population can not abide any members of the Y -population. Likewise, the most tolerant member of the Y -population can abide a $\frac{X}{Y}$ ratio of $b > 0$ and the least tolerant member of the Y -population can not abide any members of the X -population.

In the one-neighborhood problem, it is assumed that outside the neighborhood, there is a “place where color does not matter” (Schelling, 1971). Population members can move between this place and the neighborhood.

We now consider the case of two neighborhoods and two populations, where any population leaving one neighborhood must necessarily enter the other. Let $(X_i, Y_i), i = 1, 2$ denote the (X, Y) -populations in neighborhood i . So $X_1 + X_2 = X_{total}$ and $Y_1 + Y_2 = Y_{total}$ where X_{total}, Y_{total} are both constant. As above, we scale populations such that $X_{total} = 1$ and $Y_{total} = \frac{1}{k}$. Hence

$$X_2 = 1 - X_1, \quad (3)$$

$$Y_2 = \frac{1}{k} - Y_1. \quad (4)$$

If the neighborhoods were completely independent of one another, then $(X_i, Y_i), i = 1, 2$ would separately satisfy (1). But the population dynamics in one neighborhood is affected by movement of population to and from the other neighborhood. So we have to take that into account in our modeling. To do this we make the additional mild assumption that each member in both neighborhoods only cares about the population mixture of the neighborhood that they are in.

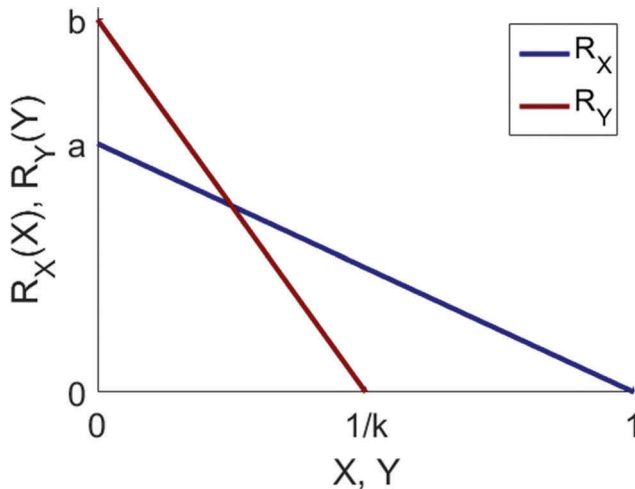


Figure 1. Linear tolerance schedules $R_X(X), R_Y(Y)$, as defined in (2).

Let us consider neighborhood 1. The dynamics is governed by the following equations.

$$\frac{dX_1}{dt} = X_1[X_1R_{X_1}(X_1) - Y_1] - X_2[X_2R_{X_2}(X_2) - Y_2] \quad (5)$$

$$\frac{dY_1}{dt} = Y_1[Y_1R_{Y_1}(Y_1) - X_1] - Y_2[Y_2R_{Y_2}(Y_2) - X_2] \quad (6)$$

The first two terms on the right hand side of (5) are the same as those in (1) and correspond to the movement of X -population, subject to the presence of the Y -population, in and out of neighborhood 1. The third and fourth terms account for the movement of the X -population, subject to the presence of the Y -population, in and out of neighborhood 2. The terms on the right hand side of (6) can be considered in an analogous way.

For linear tolerance schedules (2) in both neighborhoods, for $i = 1, 2$ we set

$$R_{X_i}(X_i) = a_i(1 - X_i), \quad (7)$$

where $(\alpha, \beta) = (7, 49)$ in general. From (3) and (4), the dynamics in neighborhood 2 is given simply by

$$\frac{dX_2}{dt} = -\frac{dX_1}{dt}, \quad (8)$$

$$\frac{dY_2}{dt} = -\frac{dY_1}{dt}. \quad (9)$$

So we have no need to consider these dynamics explicitly, since they can be obtained directly from the dynamics of neighborhood 1.

Substituting (3), (4) into (5) and (6), with linear tolerance schedules (7), we obtain the following equations for (X_1, Y_1) :

$$\frac{dX_1}{dt} = a_1X_1^2(1 - X_1) - X_1Y_1 - a_2X_1(1 - X_1)^2 + (1 - X_1)\left(\frac{1}{k} - Y_1\right), \quad (10)$$

Note that the coordinate axes $X_1 = 0, Y_1 = 0$ are no longer nullclines of the full system (unlike in Haw & Hogan, 2018).

We can reduce the ensuing algebraic complexity by performing an additional scaling. Define new variables \hat{t} , \hat{Y}_1 given by

$$\hat{t} = \frac{t}{k}, \quad \hat{Y}_1 = \frac{Y_1}{a_1} \quad (11)$$

and then set

$$\alpha = ka_1, \quad \beta_1 = a_1b_1, \quad \beta_2 = a_1b_2, \quad \gamma = \frac{a_2}{a_1}. \quad (12)$$

Now we drop the hats and simplify (10) to find:

$$\frac{dX_1}{dt} = (1 - X_1)[1 - \alpha\gamma X_1 + \alpha(1 + \gamma)X_1^2] - \alpha Y_1, \quad (13)$$

Equilibria (steady states) in neighborhood 1 are given by $(X_1, Y_1) = (X_1^e, Y_1^e)$ where $\frac{dX_1^e}{dt} = \frac{dY_1^e}{dt} = 0$. If both $X_1^e \neq 0$ and $Y_1^e \neq 0$, these equilibria correspond to integration. We find (X_1^e, Y_1^e) by considering the intersection in (X_1, Y_1) -space of the nullclines of (13), namely solutions of

$$\alpha Y_1 = (1 - X_1)[1 - \alpha Y_1 + \alpha(1 + \gamma)X_1^2], \quad (14)$$

$$X_1 = (1 - \alpha Y_1)[1 - \beta_2 Y_1 + \alpha(\beta_1 + \beta_2)Y_1^2]. \quad (15)$$

We will establish conditions under which real positive solutions of (14) and (15) can exist. Then we will find further conditions under which such solutions are stable.

Note that, in moving from (a, b, k) to (α, β) , there exists a set of systems for each (α, β) that differ only in a global scaling of time for the minority population. The parameters a and b denote the upper tolerance limits of the majority and minority populations respectively, and k defines the relative sizes of the total populations. A larger α therefore indicates a more tolerant minority; a larger β indicates a smaller minority; larger α and β indicate a more tolerant majority, or both a more tolerant and smaller minority.

2.1. Case I

We consider the case when the (X, Y) -population linear tolerance schedules are identical in both neighborhoods. So in (7), we set

$$a_1 = a_2 = a, \quad b_1 = b_2 = b,$$

Hence from (12) we have

$$\alpha = ka, \quad \beta_1 = \beta_2 = \beta, \quad \gamma = 1. \quad (16)$$

Parameters α and β are key to what follows. With scaling (11), both refer to the minority Y -population: large/small α corresponds to a small/large minority and large/small β refers to a tolerant/intolerant minority. From (13), the governing equations become

$$\frac{dX_1}{dt} = (1 - X_1)[1 - \alpha X_1 + 2\alpha X_1^2] - \alpha Y_1, \quad (17)$$

Our aim is to find how many possible equilibria (X_1^e, Y_1^e) exist and then to examine their stability. The points (X_1^e, Y_1^e) correspond to the intersection of the nullclines

$$\alpha Y_1 = (1 - X_1)[1 - \alpha X_1 + 2\alpha X_1^2], \quad (18)$$

$$X_1 = (1 - \alpha Y_1)[1 - \beta Y_1 + 2\alpha\beta Y_1^2]. \quad (19)$$

Substitution of (18) into (19) gives an equation of the form

$$p_9(X_1) = 0,$$

where $p_9(X_1)$ is a real polynomial of degree 9 in X_1 . So there are at most 9 equilibria of (17).

By inspection, we have X_2 for any values of the parameters α, β . These solutions correspond to:

$(X_1^e, Y_1^e) = (1, 0)$ all the X -population and none of the Y -population in neighborhood 1; none of the X -population and all the Y -population in neighborhood 2.

$\tilde{p}_7(X_1) \equiv \sum b_i X_1^i$. none of the X -population and all the Y -population in neighborhood 1; all the X -population and none of the Y -population in neighborhood 2.

$(X_1^e, Y_1^e) = (\frac{1}{2}, \frac{1}{2\alpha})$ both X, Y -populations evenly split between neighborhoods 1 and 2.

So we can write

$$p_9(X_1) = X_1(1 - X_1)(1 - 2X_1)p_6(X_1) \quad (20)$$

where

$$p_6(X_1) \equiv \sum_{i=0}^6 a_i X_1^i \quad (21)$$

is a real polynomial of degree 6. It can be shown that $p_6(X_1) = p_6(X_2) = p_6(1 - X_1)$, from (3). This gives $a_5 = -3a_6$, $a_3 = 5a_6 - 2a_4$, $a_1 = -3a_6 + a_4 - a_2$ and so the odd coefficients of $p_6(X_1)$ can be written in terms of the even coefficients. We find that

$$\begin{aligned} a_0 &= \alpha + \beta + \frac{\beta}{\alpha} \\ a_1 &= -3\beta(\alpha + 2) \\ a_2 &= \beta(2\alpha^2 + 15\alpha + 6) \\ a_3 &= -12\alpha\beta(\alpha + 2) \\ a_4 &= 2\alpha\beta(13\alpha + 6) \\ a_5 &= -24\alpha^2\beta \\ a_6 &= 8\alpha^2\beta. \end{aligned} \quad (22)$$

Since both $\alpha, \beta > 0$, the signs of a_i in $p_6(X_1)$ alternate. Hence by Descartes' rule of signs, $p_6(X_1)$ can have 0, 2, 4 or 6 positive real roots ($X_1 = X_1^e > 0$), depending on parameter values, and no negative real roots. By the symmetry of $p_6(X_1)$, any roots $X_1^e \in [0, 1]$. Hence $p_9(X_1)$ can have 3, 5, 7 or 9 positive real roots, no negative real roots and any roots must lie in the interval $[0, 1]$.

Note that we could have chosen to eliminate X_1 from (18) and (19) to give a ninth order polynomial $q_9(Y_1)$ in Y_1 . Similar considerations would then apply to the roots of $q_9(Y_1)$ with any roots $Y_1^e \in [0, \frac{1}{\alpha}]$.

We show examples of three qualitatively different cases in Figure 2 for $(\alpha, \beta) = (9, 16), (9, 40), (9, 80)$. On the left hand side, we show the nullclines (18), (19) in (X_1, Y_1) -space for each case. We color the basins of attraction in our plots according to the stable equilibrium which it contains³. On the right hand side of Figure 2, we plot the corresponding $p_6(X_1)$.

Figure 2a shows the case when $\alpha = 9$, $\beta = 16$. Here $p_9(X_1)$ has only three real roots corresponding to $(X_1^e, Y_1^e) = (1, 0), (0, \frac{1}{\alpha}), (\frac{1}{2}, \frac{1}{2\alpha})$. The basin of attraction of $(X_1^e, Y_1^e) = (0, \frac{1}{\alpha})$ is shown in pink and the basin of attraction of $(X_1^e, Y_1^e) = (1, 0)$ is shown in blue. The equilibrium $A\eta^6 + B\eta^4 + C\eta^2 + D = 0$ has no basin of attraction. Figure 2b shows that the corresponding $p_6(X_1)$ has no real zeros.

In Figure 2c, we take $\alpha = 9$, $\beta = 40$. Now nullclines (18), (19) have five intersections, corresponding to five real roots of $p_9(X_1)$. Three of these roots correspond to $(X_1^e, Y_1^e) = (1, 0), (0, \frac{1}{\alpha}), (\frac{1}{2}, \frac{1}{2\alpha})$, as before. So the two new roots correspond to zeros of $p_6(X_1)$. Figure 2d shows that $p_6(X_1)$ has indeed developed two zeros. Neither of these two new equilibria has a basin of attraction⁴.

In Figure 2e, we take $\alpha = 9$, $\beta = 80$. Nullclines (18), (19) have nine intersections, corresponding to nine real roots of $p_9(X_1)$ and $p_6(X_1)$ has six zeros, seen in Figure 2f. Two of these six roots correspond to integrated populations with a basin of attraction, shown in white in Figure 2e.

In this case, there is no example of $p_9(X_1)$ having seven roots, corresponding to $p_6(X_1)$ having four zeros.

³In fact, the color scheme is based on the *index of dissimilarity* (Massey & Denton, 1988) evaluated at the corresponding stable equilibrium state; see Section 5.

⁴Note that the central equilibrium $(X_1^e, Y_1^e) = (\frac{1}{2}, \frac{1}{2\alpha})$ has changed its character from a saddle in Figure 2a to an unstable node in Figure 2c. We discuss the nature of these equilibria in Section 2.1.2 below.

From a societal perspective, Figure 2 paints a rather gloomy picture. Figure 2a,c both imply that populations will be segregated at these values of (α, β) , since both figures show only basins of attraction of segregated populations. The central (integrated) equilibrium $(X_1^e, Y_1^e) = (\frac{1}{2}, \frac{1}{2\alpha})$ never has a basin of attraction and so appears unstable. Stable integration seems possible only in Figure 2e, corresponding to a small, highly tolerant, minority. As in the single-neighborhood case (Haw & Hogan, 2018), *tipping points* of the system correspond to the boundaries of the basins of attraction.

We will now establish exact criteria for the existence and stability of roots of $p_9(X_1)$ as (α, β) vary.

2.1.1. Existence of equilibria of (17)

Since we always have roots $X_1^e = 0, \frac{1}{2}, 1$ of $p_9(X_1)$, we need only consider the existence of roots of $p_6(X_1)$. From the right hand side of Figure 2, there will be at least two real roots of $p_6(X_1)$ when

$$p_6\left(\frac{1}{2}\right) < 0.$$

Since $p_6\left(\frac{1}{2}\right) = \alpha^2 - \frac{1}{2}\alpha\beta + \beta$, then $p_6\left(\frac{1}{2}\right) < 0$ implies that

$$\beta > \beta_c \equiv \frac{2\alpha^2}{\alpha - 2}. \quad (23)$$

Since $\beta > 0$, we must have $\alpha > 2$. At $\beta = \beta_c$, the two nullclines (18), (19) have a cubic tangency. Note the minimum value of $\beta_c = 16$, which occurs when $\alpha = 4$. The next step is to observe that if $X_1 = \frac{1}{2} + \eta$ is a root of $p_6(X_1) = 0$, then by symmetry, so too is $X_1 = \frac{1}{2} - \eta$, where $\eta \in [0, \frac{1}{2}]$. So we have two equations for η :

$$\sum_{i=0}^6 a_i \left(\frac{1}{2} \pm \eta\right)^i = 0, \quad (24)$$

where a_i , $i = 0 \dots 6$ are given in (22). We now expand both equations in (24), and add to give

$$A\eta^6 + B\eta^4 + C\eta^2 + D = 0 \quad (25)$$

where

$$A = 8\alpha^2\beta, \quad (26)$$

$$B = 4\alpha\beta(3 - \alpha), \quad (27)$$

$$C = \frac{1}{2}\beta(\alpha^2 - 6\alpha + 12), \quad (28)$$

$$D = \alpha - \frac{\beta}{2} + \frac{\beta}{\alpha}. \quad (29)$$

So η^2 has either one or three real values, depending on the sign of the discriminant $\Delta \equiv B^2C^2 - 4AC^3 - 4B^3D - 27A^2D^2 + 18ABCD$, because (25) is a cubic in η^2 . Hence $p_6(X_1)$ will have either two real roots or six real roots; it can not have four real roots. Hence $p_9(X_1) = 0$ can not have seven roots (the missing case from Figure 2). Note that this is not in contradiction of Descartes' rule of signs, which is a necessary condition only. Note that when $D = 0$, we have $\beta = \beta_c$ and (25) has solution $\eta^2 = 0$. Hence $p_6(\frac{1}{2}) = 0$, which corresponds exactly to (23).

A lengthy calculation shows that

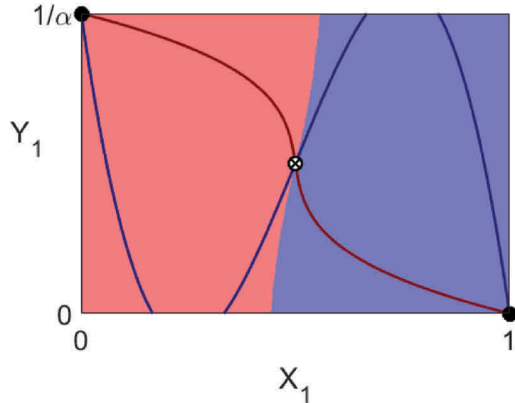
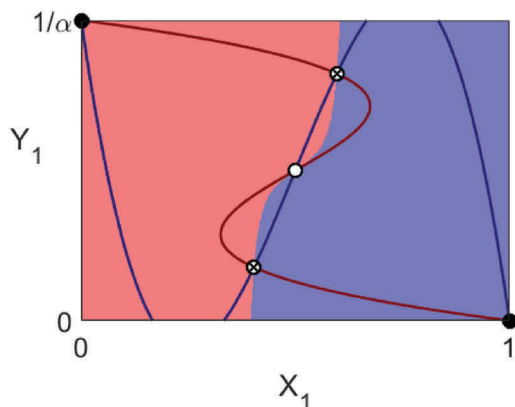
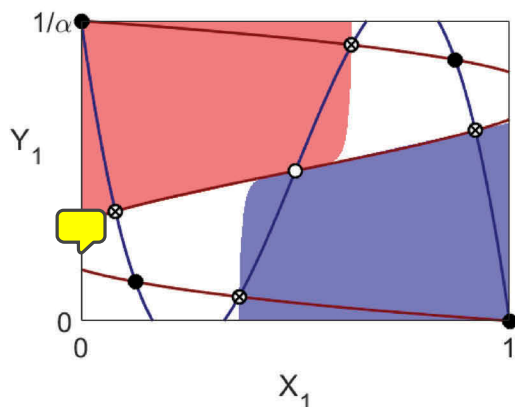
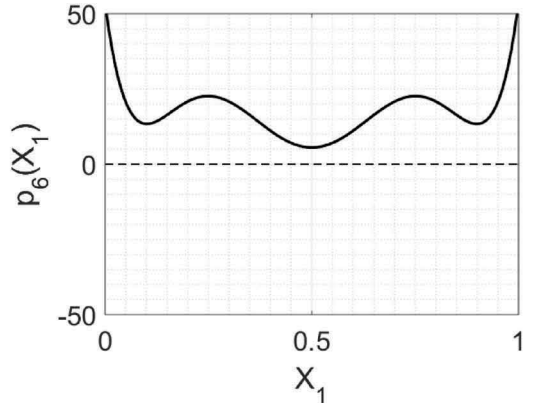
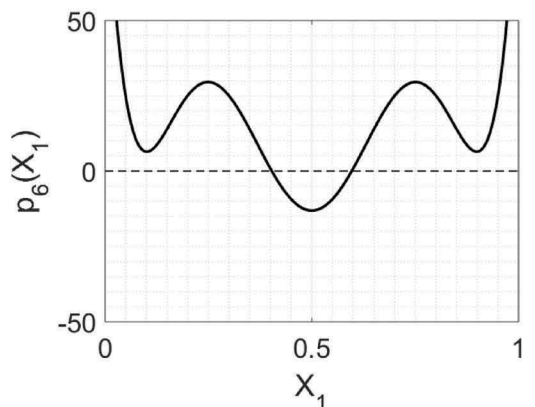
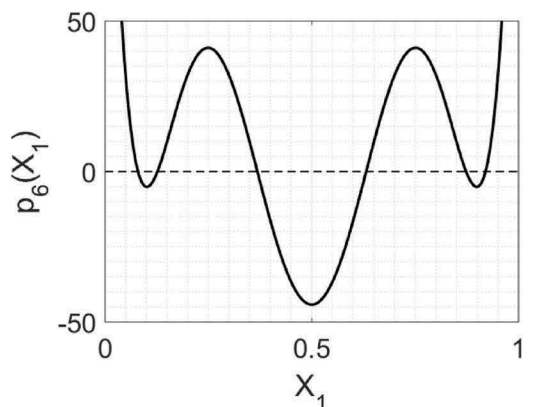
(a) $\alpha = 9, \beta = 16$: (X_1, Y_1) phase space(c) $\alpha = 9, \beta = 40$: (X_1, Y_1) phase space(e) $\alpha = 9, \beta = 80$: (X_1, Y_1) phase space(b) $\alpha = 9, \beta = 16$: $p_6(X_1)$ vs X_1 (d) $\alpha = 9, \beta = 40$: $p_6(X_1)$ vs X_1 (f) $\alpha = 9, \beta = 80$: $p_6(X_1)$ vs X_1

Figure 2. Three qualitatively different possibilities for Case I. In the left hand figures, nullcline (18) is shown in blue and nullcline (19) is shown in red. The pink region is the basin of attraction of the equilibrium $(X_1^e, Y_1^e) = (0, \frac{1}{\alpha})$ and the blue region is the basin of attraction of $(X_1^e, Y_1^e) = (1, 0)$. The white regions in Figure 2e correspond to the basin of attraction of two of the new equilibria in that figure. Stable nodes are denoted by \bullet , unstable nodes by \circ and saddle points by \otimes . The right hand figures show $p_6(X_1)$ in each case.

$$\Delta = -4\alpha^5\beta^2[8\alpha^2\beta + \alpha(432 - 72\beta - \beta^2) + 8\beta^2]. \quad (30)$$

Hence $\Delta = 0$ when $\beta = \beta_{\pm}$ where

$$\beta_{\pm} \equiv \frac{4}{8-\alpha} \left[9\alpha - \alpha^2 \pm \sqrt{\alpha(\alpha-6)^3} \right]. \quad (31)$$

So η^2 has three real values, and η has six real values, for $\beta \in [\beta_-, \beta_+]$. At $\beta = \beta_{\pm}$, the two nullclines (18), (19) have quadratic tangencies. We must have $\alpha \geq 6$ for real values of β_{\pm} .

The existence of equilibria of (17) is summarized in [Figure 3](#). Solid lines correspond to $\beta = \beta_c \equiv 2\alpha^2/(\alpha-2)$, from (23) and $\beta = \beta_{\pm} \equiv \frac{4}{8-\alpha} \left[9\alpha - \alpha^2 \pm \sqrt{\alpha(\alpha-6)^3} \right]$, from (31). The apex of the dark shaded region is the point $P_2 = (\alpha, \beta) = (6, 36)$. Since integrated equilibria occur only inside this region, we can deduce that this version of the two-room problem requires a very tolerant (large β), small (large α) minority to produce an integrated population (which may or may not be stable). Candidate values for (a, b, k) at the apex P_2 include $(3, 6, 3)$ and $(6, 6, 1)$ (c.f. discussion for comparison with the single neighborhood model).

The above analysis also allows us to obtain an exact expansion of $p_6(X_1)$ as a cubic in $(X_1 - \frac{1}{2})$. Since $\eta = \pm(X_1 - \frac{1}{2})$, we have from (24) and (25) that

$$p_6(X_1) = \sum_{i=0}^6 a_i X_1^i \quad (32)$$

$$= A \left(X_1 - \frac{1}{2} \right)^6 + B \left(X_1 - \frac{1}{2} \right)^4 + C \left(X_1 - \frac{1}{2} \right)^2 + D. \quad (33)$$

So

$$\begin{aligned} p_9(X_1) &= X_1(1-X_1)(1-2X_1) \left[8\alpha^2\beta \left(X_1 - \frac{1}{2} \right)^6 + 4\alpha\beta(3-\alpha) \left(X_1 - \frac{1}{2} \right)^4 \right. \\ &\quad \left. + \frac{1}{2}\beta(\alpha^2 - 6\alpha + 12) \left(X_1 - \frac{1}{2} \right)^2 + \left(\alpha - \frac{\beta}{2} + \frac{\beta}{\alpha} \right) \right]. \end{aligned} \quad (34)$$

Hence we can give exact expressions for all the roots $X_1 = X_1^e$ of $p_9(X_1) = 0$. We already have $X_1^e = 0, \frac{1}{2}, 1$. Now we can solve $p_6(X_1^e) = 0$ for $(X_1^e - \frac{1}{2})^2$ from (34) using the standard formula for roots of a cubic, take the square root and obtain X_1^e and then use (18) to obtain the corresponding value of Y_1^e . These unwieldy expressions, not given here, can then be used to check the numerical results in [Figure 2](#).

2.1.2. Stability of equilibria of (17)

It is clear from [Figure 2](#) that not all equilibria of (17) are stable, since they have no basin of attraction. In this section, we determine stability criteria for equilibria of (17). Let us write (17) in the form

$$\begin{aligned} \frac{dX_1}{dt} &= P(X_1, Y_1), \\ a_1 \frac{dY_1}{dt} &= Q(X_1, Y_1). \end{aligned} \quad (35)$$

where

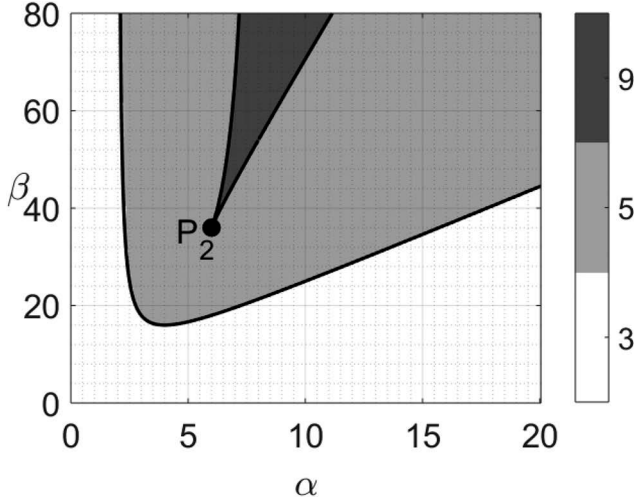


Figure 3. Number of equilibria of (17), corresponding to the roots of $p_9(X_1)$. Solid lines correspond to $\beta = \beta_c \equiv 2\alpha^2/(\alpha - 2)$, from (23) and $\beta = \beta_{\pm} \equiv \frac{4}{8-\alpha} [9\alpha - \alpha^2 \pm \sqrt{\alpha(\alpha - 6)^3}]$, from (31). Integrated equilibria occur only inside the dark shaded region, for $\beta \in [\beta_-, \beta_+]$, when (17) has nine equilibria. The polynomial $p_9(X_1)$ has five roots in the light shaded region and only three roots in the white shaded region. In both these cases, only segregated equilibria are possible. The apex P_2 of the dark shaded region is the point $(\alpha, \beta) = (6, 36)$.

$$\begin{aligned} P(X_1, Y_1) &= (1 - X_1)[1 - \alpha X_1 + 2\alpha X_1^2] - \alpha Y_1, \\ Q(X_1, Y_1) &= (1 - \alpha Y_1)[1 - \beta Y_1 + 2\alpha\beta Y_1^2] - X_1. \end{aligned} \quad (36)$$

To establish stability criteria, we must calculate the eigenvalues of the Jacobian of (35), given by

$$J(X_1, Y_1) \equiv \begin{pmatrix} \frac{\partial P}{\partial X_1} & \frac{\partial P}{\partial Y_1} \\ \frac{\partial Q}{\partial X_1} & \frac{\partial Q}{\partial Y_1} \end{pmatrix} = \begin{pmatrix} -(1 + \alpha) + 6\alpha X_1(1 - X_1) & -\alpha \\ -1 & -(\alpha + \beta) + 6\alpha\beta Y_1(1 - \alpha Y_1) \end{pmatrix}, \quad (37)$$

evaluated at the various equilibria $(X_1, Y_1) = (X_1^e, Y_1^e)$.

For the equilibrium $(X_1^e, Y_1^e) = (1, 0)$, the eigenvalues of $J(X_1, Y_1)$ are given by

$$\lambda_{\pm} = \frac{1}{2} \left[-(1 + 2\alpha + \beta) \pm \sqrt{4\alpha + (1 - \beta)^2} \right]. \quad (38)$$

It is straightforward to show that both $\lambda_{\pm} < 0$ for all $\alpha > 0, \beta > 0$. Hence the equilibrium $(X_1^e, Y_1^e) = (1, 0)$, corresponding to all of the X-population in neighborhood 1 and all of the Y-population in neighborhood 2, is a stable node, shown by a solid circle (\bullet) in Figure 2. Unless the system is modified in some way, this means that there will always be a non-empty set of initial conditions that will lead to this segregated outcome.

For the equilibrium $(X_1^e, Y_1^e) = (0, \frac{1}{\alpha})$, the eigenvalues are also given by (38). Similar considerations apply to this (stable) segregated outcome.

The equilibrium $(X_1^e, Y_1^e) = (\frac{1}{2}, \frac{1}{2\alpha})$ has a more subtle behavior. Its eigenvalues are given by

$$\lambda_{\pm} = \frac{1}{4} \left[\beta - (\alpha + 2) \pm \sqrt{(\beta + 2)^2 + 9\alpha^2 + 4\alpha - 6\alpha\beta} \right]. \quad (39)$$

We can show that $\lambda_+ > 0$ in (39). Hence the equilibrium is always unstable. In addition, $\lambda_- \geq 0$ for $\beta \geq \beta_c$ where $\beta_c \equiv 2\alpha^2/(\alpha - 2)$, from (23). Hence $(X_1^e, Y_1^e) = (\frac{1}{2}, \frac{1}{2\alpha})$ is a saddle for $\beta < \beta_c$, shown by a crossed circle (\otimes) in Figure 2, and an unstable node for $\beta > \beta_c$, shown by an open circle (\circ). At

$\beta = \beta_c$, we have a supercritical pitchfork bifurcation, where the saddle at $(X_1^e, Y_1^e) = (\frac{1}{2}, \frac{1}{2\alpha})$ becomes an unstable node and two saddles. This explains why no new stable equilibria are created at $\beta = \beta_c$. This bifurcation occurs precisely at the boundary between three and five equilibria shown in Figure 3.

The three equilibria considered so far are zeros of $p_9(X_1)$; they always exist for any values of α, β . The remaining zeros of $p_9(X_1)$ come from $p_6(X_1)$. They can be found analytically, as explained above. But the expressions for the equilibria are unwieldy and the ensuing stability calculations are extremely lengthy. So we will simply summarize the results.

In Figure 4a, we set $\alpha = 1.9$ and plot the resulting values of X_1^e as a function of β (the values of Y_1^e are omitted, for convenience). Since $\alpha < 2$, none of the quantities β_c, β_{\pm} is defined and $p_9(X_1)$ only has three real zeros: $X_1^e = 0, 1$ (both stable nodes, shown in green) and $X_1^e = \frac{1}{2}$ (a saddle, shown in black).

In Figure 4b, we take $\alpha = 5$. Since $2 < \alpha < 6$, we have $\beta_c = \frac{50}{3} \approx 16.67$, with β_{\pm} undefined. The saddle existing for $\beta < \beta_c$ becomes an unstable node (shown in red) and the new solutions for $\beta > \beta_c$ are saddles.

In Figure 4c, we set $\alpha = 7.1$. Hence $\beta_c \approx 19.77$ and $\beta_- \approx 46.29, \beta_+ \approx 73.62$. The pitchfork bifurcation at $\beta = \beta_c$ is followed by fold bifurcations at $\beta = \beta_{\pm}$. For $\beta \in [\beta_-, \beta_+]$, we see two stable nodes, corresponding to stable integration. These two solution branches have different basins of attraction (see Figure 2e).

Finally in Figure 4d, $\alpha = 10$ and now the pitchfork bifurcation is at $\beta = \beta_c = 25$. We can always find an integrated population whenever $\beta > \beta_- \approx 70.60$.

So to get a stable integration in two neighborhoods with the same linear tolerance schedules, we need to select parameters (α, β) to lie in the dark shaded region of Figure 3, corresponding to a small, highly tolerant, minority. For $6 < \alpha < 8$, we can only find an integrated solution when $\beta_- < \beta < \beta_+$. For $\alpha > 8$, we can always find an integrated population whenever $\beta > \beta_-$, provided we start with the right initial conditions.

2.2. Case II, III and IV

In the previous section, the linear tolerance schedules (7) were the same in both neighborhoods ($\gamma = 1, \beta_1 = \beta_2$) for both majority X - and minority Y -populations. Let us now consider the case in which the linear tolerance schedules are different. The types of people remain the same, but the two neighborhoods induce a different tolerance in each population (this may be due to other factors such as urban environment, educational provision, etc). We revert to the original dynamical system (13) and nullclines (14) and (15). We distinguish three different cases:

Case II; $\gamma = 1, \beta_1 \neq \beta_2$: the majority population have the same tolerance in both neighborhoods; the minority have different tolerances in both neighborhoods.

Case III; $\gamma \neq 1, \beta_1 = \beta_2$: the majority population have different tolerances in both neighborhoods; the minority have the same tolerance in both neighborhoods.

Case IV; $\gamma \neq 1, \beta_1 \neq \beta_2$: both populations have different tolerances in both neighborhoods.

Substituting (14) into (15), we obtain a ninth order polynomial $\tilde{p}_9(X_1)$ of possible equilibria. We know that $X_1^e = 0, 1$, by inspection of (14), (15). But $X_1^e = \frac{1}{2}$ is no longer a guaranteed equilibrium. Hence we write

$$\tilde{p}_9(X_1) = X_1(1 - X_1)\tilde{p}_7(X_1),$$

where

$$\tilde{p}_7(X_1) \equiv \sum_{i=0}^7 b_i X_1^i. \quad (40)$$

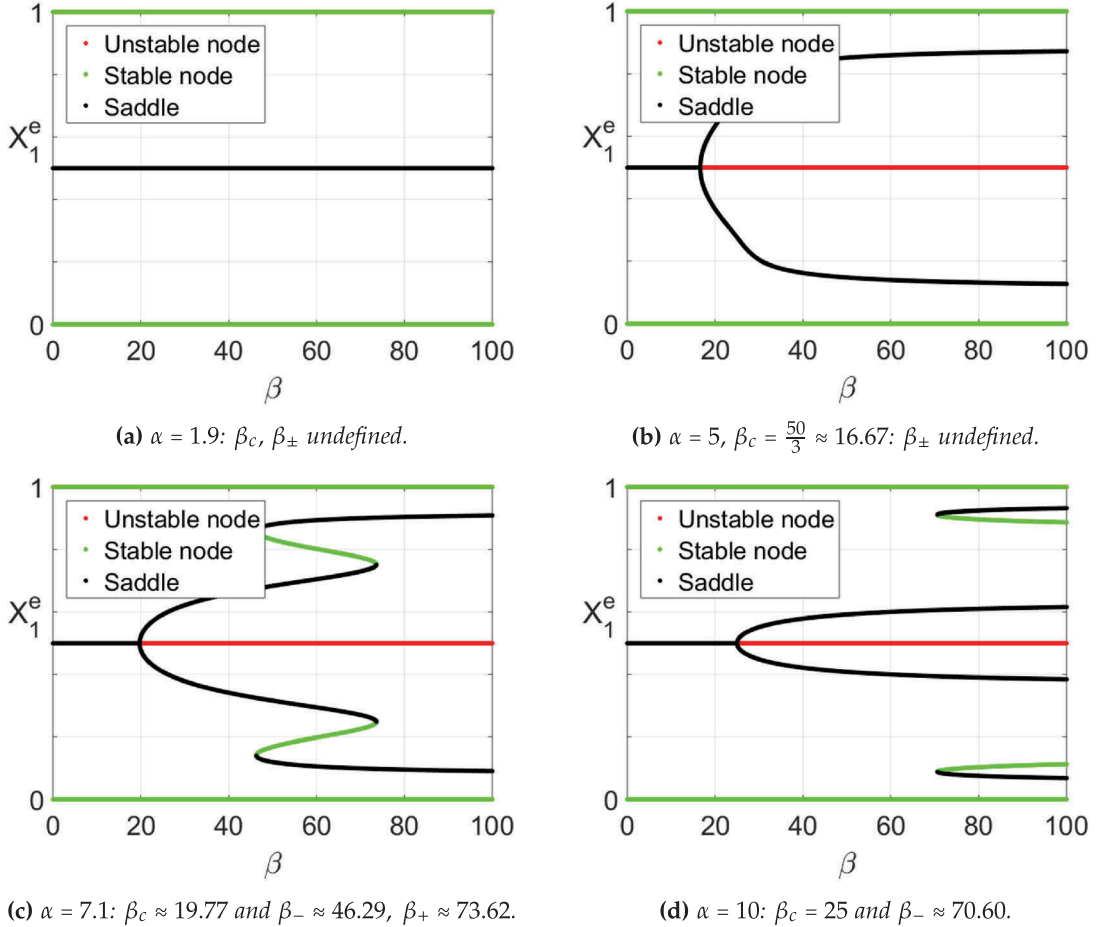


Figure 4. Case I: equilibrium values X_1^e as a function of β for (a) $\alpha = 1.9$, (b) $\alpha = 5$, (c) $\alpha = 7.1$ and (d) $\alpha = 10$.

The real coefficients b_i are given by

$$b_0 = -(\alpha + \beta_1)\gamma - \frac{\beta_1}{\alpha} \quad (41)$$

$$b_1 = \left(1 + \frac{1}{\alpha}\right)\beta_1 + \alpha(1 + \gamma) + \frac{\beta_2}{\alpha} + (5\beta_1 + 2\beta_2)\gamma + \alpha(2\beta_1 + \beta_2)\gamma^2$$

$$b_2 = -2(2\beta_1 + \beta_2) - [(7 + 4\alpha)\beta_1 + (5 + 2\alpha)\beta_2]\gamma - 3\alpha(3\beta_1 + 2\beta_2)\gamma^2 - \alpha^2(\beta_1 + \beta_2)\gamma^3$$

$$b_3 = (3 + 2\alpha)\beta_1 + (3 + \alpha)\beta_2 + [(3 + 14\alpha)\beta_1 + (3 + 10\alpha)\beta_2]\gamma + [3\alpha(5 + \alpha)\beta_1 + 3\alpha(4 + \alpha)\beta_2]\gamma^2 + 5\alpha^2(\beta_1 + \beta_2)\gamma^3$$

$$b_4 = -\alpha(5\beta_1 + 4\beta_2) - \alpha[(16 + 3\alpha)\beta_1 + (14 + 3\alpha)\beta_2]\gamma - \alpha[(11 + 12\alpha)\beta_1 + (10 + 12\alpha)\beta_2]\gamma^2 - 10\alpha^2(\beta_1 + \beta_2)\gamma^3$$

$$b_5 = \alpha(\beta_1 + \beta_2)[3 + \alpha + 3(2 + 3\alpha)\gamma + 3(1 + 6\alpha)\gamma^2 + 10\alpha\gamma^3]$$

$$b_6 = -\alpha^2(\beta_1 + \beta_2)(2 + 9\gamma + 12\gamma^2 + 5\gamma^3)$$

$$b_7 = \alpha^2(\beta_1 + \beta_2)(1 + \gamma)^3$$

Note that $\tilde{p}_7(X_1)$ evaluated at $\gamma = 1$, $\beta_1 = \beta_2$ can be shown to equal $(1 - 2X_1)p_6(X_1)$, as expected.

2.2.1. Equilibria

Equilibria of the governing Equations (13), segregated or integrated, correspond to real zeros of $\tilde{p}_9(X_1)$. We know by inspection that $X^e = 0, 1$ are equilibria. But owing to the lack of symmetry between the two neighborhoods, we can say very little analytically about any other equilibria, corresponding to real zeros of $\tilde{p}_7(X_1)$ in (40).

The signs of the coefficients b_i of $\tilde{p}_7(X_1)$ alternate for allowed values of the parameters. So Descartes' rule of signs tells us that $\tilde{p}_7(X_1)$ has 1,3,5 or 7 real roots for $X_1 > 0$ and no real roots for $X_1 < 0$. Hence $\tilde{p}_9(X_1)$ has 3, 5, 7 or 9 real roots for $X_1 > 0$ and no real roots for $X_1 < 0$, as in case I.

We can also show that there has to be at least one real root of $\tilde{p}_7(X_1)$ for $X_1 \in (0, 1)$, for any allowed parameter values. Simple calculation shows that $\tilde{p}_7(0) = -(\alpha + \beta_1)\gamma - \frac{\beta_1}{\alpha} < 0$ and $\tilde{p}_7(1) = (\alpha + \beta_2) + \frac{\beta_2}{\alpha} > 0$. Since $\tilde{p}_7(X_1)$ is continuous in X_1 , the Intermediate Value Theorem tells us that there always has to be at least one zero of $\tilde{p}_7(X_1)$ between $X_1 = 0$ and $X_1 = 1$. Since neither $\tilde{p}_7(1)$ nor $\tilde{p}_7(0)$ is identically zero, the root must lie strictly between $X_1 = 0$ and $X_1 = 1$.

Governing Equations (13) can be written in the form

$$\begin{aligned} \frac{dX_1}{dt} &= K(X_1, Y_1), \\ a_1 \frac{dY_1}{dt} &= L(X_1, Y_1). \end{aligned} \tag{42}$$

where

$$K(X_1, Y_1) = (1 - X_1)[1 - \alpha\gamma X_1 + \alpha(1 + \gamma)X_1^2] - \alpha Y_1, \tag{43}$$

$$L(X_1, Y_1) = (1 - \alpha Y_1)[1 - \beta_2 Y_1 + \alpha(\beta_1 + \beta_2)Y_1^2] - X_1.$$

The Jacobian of (42) is given by

$$\begin{aligned} J(X_1, Y_1) &\equiv \begin{pmatrix} \frac{\partial K}{\partial X_1} & \frac{\partial K}{\partial Y_1} \\ \frac{\partial L}{\partial X_1} & \frac{\partial L}{\partial Y_1} \end{pmatrix} \\ &= \begin{pmatrix} -(1 + \alpha\gamma) + 2\alpha(1 + 2\gamma)X_1 - 3\alpha(1 + \gamma)X_1^2 & -\alpha \\ -1 & -(\alpha + \beta_2) + 2\alpha(\beta_1 + 2\beta_2)Y_1 - 3\alpha^2(\beta_1 + \beta_2)Y_1^2 \end{pmatrix}. \end{aligned} \tag{44}$$

For the equilibrium $(X_1^e, Y_1^e) = (1, 0)$, the eigenvalues of $J(X_1, Y_1)$ are given by

$$\lambda_{\pm} = \frac{1}{2} \left[-(1 + 2\alpha + \beta_2) \pm \sqrt{4\alpha + (1 - \beta_2)^2} \right]. \tag{45}$$

Both $\lambda_{\pm} < 0$ and are independent of β_1 . Hence $(X_1^e, Y_1^e) = (1, 0)$ is always a stable node. When $\gamma = 1$, $\beta_1 = \beta_2 = \beta$, (45) reduces to (38).

For the equilibrium $(X_1^e, Y_1^e) = (0, \frac{1}{\alpha})$, the eigenvalues of $J(X_1, Y_1)$ are given by

$$\lambda_{\pm} = \frac{1}{2} \left[-(1 + \beta_1) - \alpha(1 + \gamma) \pm \sqrt{\alpha^2(\gamma - 1)^2 + (\beta_1 - 1)^2 + 2\alpha[(\gamma + 1) + \beta_1(1 - \gamma)]} \right]. \quad (46)$$

These eigenvalues are both negative for all allowed values of α, β and are independent of β_2 . Hence $(X_1^e, Y_1^e) = (0, \frac{1}{\alpha})$ is always a stable node. Equation (46) reduces to (38) when $\gamma = 1$, $\beta_1 = \beta_2 = \beta$.

Our considerations above show that there is always at least one other equilibrium of (42) in addition to $(X_1^e, Y_1^e) = (1, 0)$, $(0, \frac{1}{\alpha})$. In the case when there is exactly one additional equilibrium, the fact that both $(X_1^e, Y_1^e) = (1, 0)$, $(0, \frac{1}{\alpha})$ are always stable nodes means that this third equilibrium must be a saddle.

In general, owing to the lack of symmetry, further equilibria must be created by fold bifurcations. These happen when turning points of $\tilde{p}_7(X_1)$ (locally quadratic maxima or minima) cross the X_1 axis. We do not expect pitchfork bifurcations in case II, III or IV, which occur in systems with an inversion or reflection symmetry (Guckenheimer & Holmes, 1997), for example case I.

Fold bifurcations produce either a stable node (a desirable outcome because $X_1^e \neq 0$ and $Y_1^e \neq 0$) and a new saddle or an unstable node and a new saddle. We then face the following possibilities: (i) further equilibria (stable or unstable) can be produced by additional new fold bifurcations, (ii) the original saddle can disappear in a fold bifurcation with the newly created node or (iii) the original fold bifurcation can be reversed.

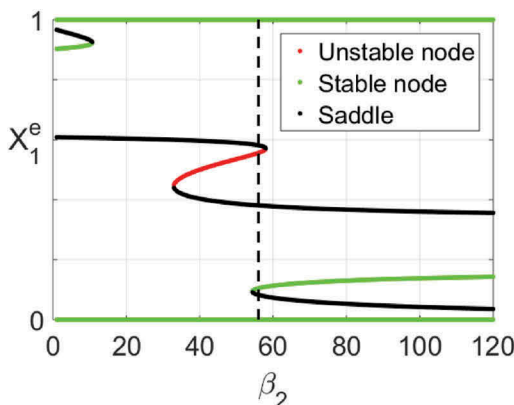
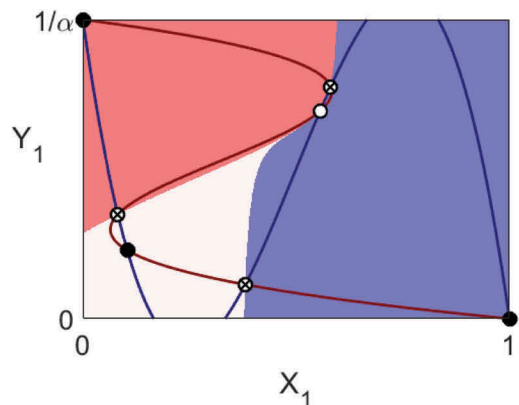
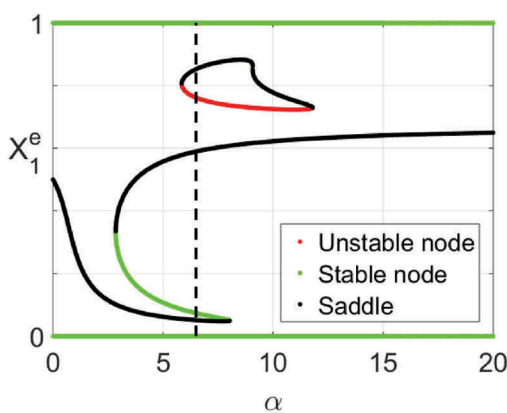
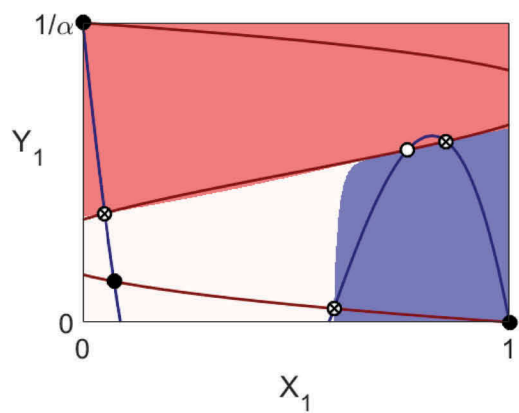
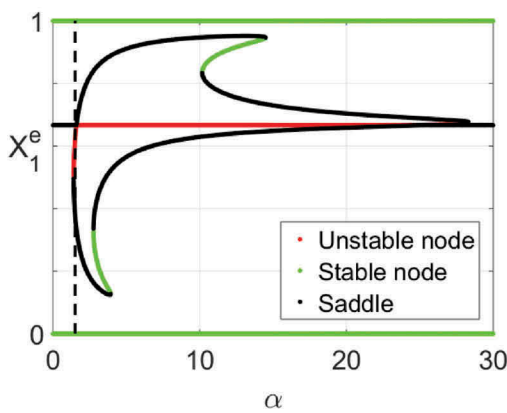
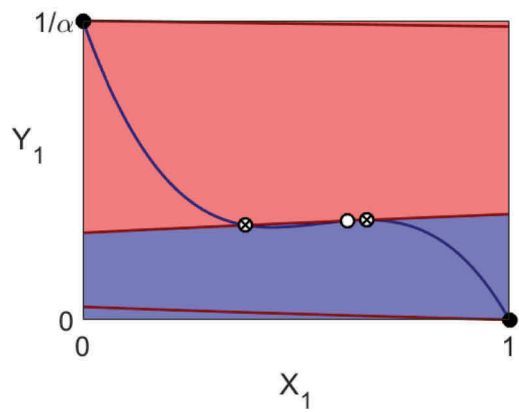
Finally in this section, we show some bifurcation diagrams to illustrate the wealth of possible behavior that can occur. For case II, $\gamma = 1$, $\beta_1 \neq \beta_2$, we take $\alpha = 9$, $\beta_1 = 40$ and vary β_2 , shown in Figure 5a. The phase space diagram for $\beta_2 = 56$ is shown in Figure 5b. For case III, $\gamma \neq 1$, $\beta_1 = \beta_2$, we take $\gamma = 2$, $\beta_1 = \beta_2 = 60$ and vary α , shown in Figure 5c. The phase space diagram for $\alpha = 6.5$ is shown in Figure 5d. Finally for case IV, $\gamma \neq 1$, $\beta_1 \neq \beta_2$, we take $\gamma = 2$, $\beta_1 = 80$, $\beta_2 = 40$ and vary α , as shown in Figure 5e. Note the presence of a transcritical bifurcation near $\alpha = 1.5$, which arises due to local symmetry. The phase space diagram for $\alpha = 1.5$ is shown in Figure 5f.

3. Limiting numbers

For the case of a single neighborhood, when parameters α, β are such that only segregation is possible, Schelling (Schelling, 1969, 1971) proposed that an integrated population could be obtained by limiting numbers of one or both populations. In (Haw & Hogan, 2018), we gave exact conditions under which this could occur. We also analyzed the stability of the resulting equilibria and showed that the removal of the most intolerant individuals can lead to integration for most values of α, β . For some parameter values, it is possible to create up to seven new equilibria. But there are some values of α, β where limitation of the population can not produce integration.

In this section, we consider how limiting numbers might affect the population mixture for two neighborhoods in case I (cases II, III and IV can be treated similarly). The picture is considerably more complicated than the one neighborhood case. There are at least two ways to limit the population when there is more than one neighborhood. We can restrict the overall number of one population. So for example, we could take $X_1 + X_2 = u$ for $u \in (0, 1)$. This is equivalent to the solution proposed by Schelling (Schelling, 1969, 1971) in the case of one neighborhood. Note that this is not the same as a simple rescaling the X -population, since the least tolerant member of the X -population can now abide a $\frac{Y}{X}$ ratio of $(1 - u) \neq 0$.

Another way to restrict population when there is more than one neighborhood is to impose a limit in one neighborhood only, for example $X_1 = u < 1$, but keep the overall population unchanged. Consequently in this case $X_2 \in [1 - u, 1]$, since $X_1 + X_2 = 1$ from (3). This way of

(a) Case II: $\gamma = 1$, $\beta_1 \neq \beta_2$; $\alpha = 9$, $\beta_1 = 40$.(b) Case II with $\alpha = 9$, $\beta_1 = 40$, $\beta_2 = 56$.(c) Case III: $\gamma \neq 1$, $\beta_1 = \beta_2$; $\gamma = 2$, $\beta_1 = \beta_2 = 60$.(d) Case III with $\gamma = 2$, $\beta_1 = \beta_2 = 60$, $\alpha = 6.5$.(e) Case IV: $\gamma \neq 1$, $\beta_1 \neq \beta_2$; $\gamma = 2$, $\beta_1 = 80$, $\beta_2 = 40$.(f) Case IV with $\gamma = 2$, $\beta_1 = 80$, $\beta_2 = 40$, $\alpha = 1.5$.**Figure 5.** Bifurcation diagrams and example phase portraits for case II, III and IV. Stable equilibria are denoted by ●, unstable nodes by ○ and saddle points by ⊗.

limiting population is different to that treated by Schelling (Schelling, 1969, 1971) and (Haw & Hogan, 2018), so we will analyze it here.

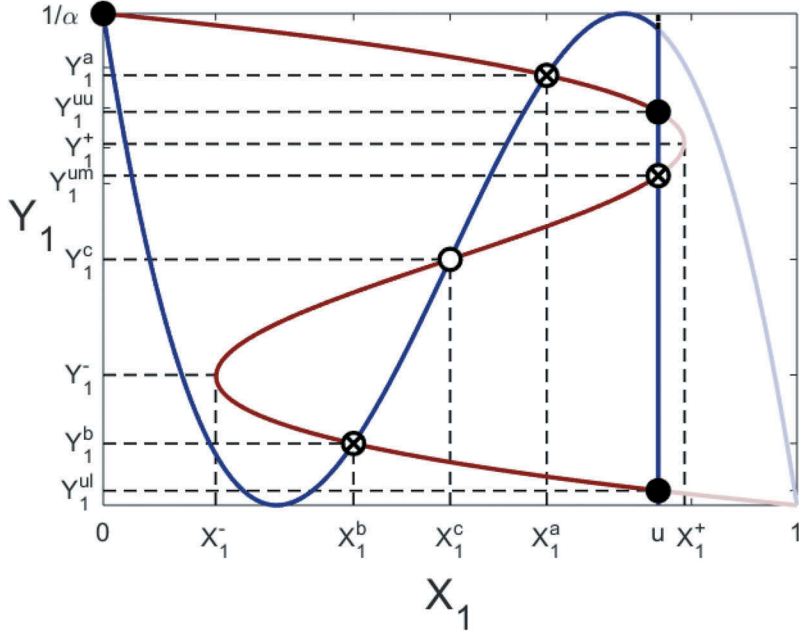


Figure 6. Limiting the X_1 population: $X_1 = u$: $\beta \in [2\alpha, 8\alpha]$, $Y_1^a > Y_1^+$.

Let us begin by restricting the X_1 -population (and hence the X_2 -population), as illustrated in Figure 6.

The Y -population is not restricted. Additional integrated will correspond to intersections of the line $X_1 = u$ with the cubic nullcline (19) given by $X_1 = (1 - \alpha Y_1)[1 - \beta Y_1 + 2\alpha\beta Y_1^2]$. In Figure 6, we show the case $\beta \in [2\alpha, 8\alpha]$, when nullcline (19) has a middle branch, which lies completely within the feasible (X_1, Y_1) phase plane. In the absence of any population restriction, there will be three integrated equilibria, given by $(X_1, Y_1) = (X_1^e, Y_1^e) = (X_1^a, Y_1^a), (X_1^c, Y_1^c), (X_1^b, Y_1^b)$.

The turning points (X_1^\pm, Y_1^\pm) of nullcline (19) are important. If the X -population is restricted at $X_1 = u$, we exclude the most intolerant people. But for $u \in [X_1^+, 1]$, we do not gain any extra equilibria. Instead the segregated equilibrium at $(X_1, Y_1) = (0, 1)$ becomes the (slightly) integrated equilibrium $(X_1, Y_1) = (u, Y_1^{ul})$.

Figure 6 shows the case when the upper unrestricted equilibrium $Y_1^a > Y_1^+$ with $u \in [X_1^a, X_1^+]$. There are three new equilibria, denoted by $(X_1, Y_1) = (u, Y_1^{ul}), (u, Y_1^{um}), (u, Y_1^{uu})$ on the lower, middle and upper branches, respectively, where $Y_1 = Y_1^{u(l,m,u)}$ are the real roots of the cubic equation

$$u = (1 - \alpha Y_1)[1 - \beta Y_1 + 2\alpha\beta Y_1^2] \quad (47)$$

when the discriminant of (47) is positive. Note that if $Y_1^a < Y_1^+$, we can only get two new equilibria if $u \in [X_1^a, X_1^+]$ (not shown).

So to proceed we must first find out when the turning points (X_1^\pm, Y_1^\pm) of nullcline (19) exist. Then since the case $Y_1^a = Y_1^+$ (and hence by symmetry⁵ $Y_1^b = Y_1^-$) separates different types of behavior, we must investigate when the two nullclines (18), (19) intersect there.

Turning points (X_1^\pm, Y_1^\pm) of nullcline (19) exist when it has a vertical tangent. From (19), we find

$$\frac{dY_1}{dX_1} = \frac{1}{[-(\alpha + \beta) + 6\alpha\beta Y_1 - 6\alpha^2\beta Y_1^2]} \quad (48)$$

⁵In cases II, III and IV, there will be two different intersections, due to the lack of symmetry.

It is straightforward to show that, when $\beta > 2\alpha$, the nullcline (19) has vertical tangents at

$$(X_1^\pm, Y_1^\pm) = \left(\frac{1}{2} \pm \frac{1}{18\alpha\beta} \sqrt{3\beta(\beta - 2\alpha)^3}, \frac{1}{2\alpha} \pm \frac{1}{6\alpha\beta} \sqrt{3\beta(\beta - 2\alpha)} \right). \quad (49)$$

When $\beta \in [2\alpha, 8\alpha]$, these vertical tangents lie within the feasible (X_1, Y_1) -plane. When $\beta = 2\alpha$, the two nullclines (18), (19), have a cubic tangency at the central equilibrium $(X_1, Y_1) = (X_1^c, Y_1^c) = (X_1^+, Y_1^+) = (X_1^-, Y_1^-) = (\frac{1}{2}, \frac{1}{2\alpha})$.

Let us now investigate ways in which equilibria can occur on the middle branch of nullcline (19), when $\beta \in [2\alpha, 8\alpha]$. Our aim is to find a curve $\Gamma_u(\alpha, \beta) = 0$ that separates regions where three integrated equilibria are possible from regions where two integrated equilibria are possible. Points on this curve must satisfy:

$$X_1^\pm \equiv \frac{1}{2} \pm \frac{1}{18\alpha\beta} \sqrt{3\beta(\beta - 2\alpha)^3} = u, \quad (50)$$

$$\alpha Y_1^\pm \equiv \frac{1}{2} \pm \frac{1}{6\beta} \sqrt{3\beta(\beta - 2\alpha)} = (1 - u)(1 - \alpha u + 2\alpha u^2). \quad (51)$$

Equation (50) is the statement that the lines $X_1 = u$ and $X_2 = 1 - u$ intersect, due to symmetry, the vertical tangents of nullcline (19). Equation (51) is the statement that points (u, Y_1^\pm) lie on nullcline (19).

Substituting (50) into (51), it can be shown that

$$\Gamma_u(\alpha, \beta) \equiv \beta^3 - 9\alpha\beta^2 + 6\alpha(\alpha + 9)\beta + 16\alpha^3. \quad (52)$$

The curve $\Gamma_u(\alpha, \beta) = 0$ is shown by the black dashed line in Figure 7a. Note that it is asymptotic to $\beta = \beta_c$ and $\beta = \beta_-$, as $\alpha \rightarrow \infty$.

Also shown in the same figure are $\beta = \beta_c$ (equation (23), shown in red); $\beta = \beta_\pm$ (Equation (31), shown in green), together with the lines $\alpha = 2$, $\alpha = 8$ and $\beta = 2\alpha$, $\beta = 8\alpha$ (shown in blue). We can see that the (α, β) parameter space is then divided up into 19 regions (some of which are extremely small). In each of these regions, the effect of restricting the X_1 -population is slightly different. We shall discuss below the behavior in two of these regions, labeled A and B in Figure 7a.

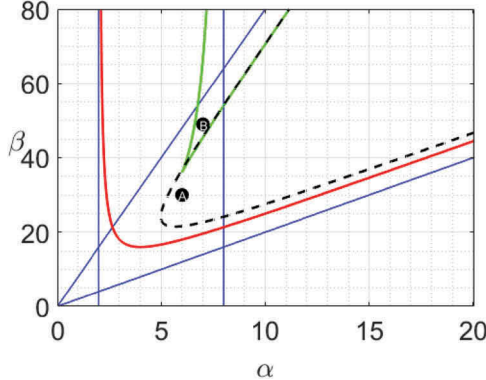
Let us now consider the case when we limit the Y_1 -population (and hence the Y_2 -population), but not the X -population. New integrated equilibria will correspond to intersections of the line $Y_1 = v$ with the cubic nullcline (18), given by solutions $Y_1 = Y_1^v$ of $\alpha Y_1 = (1 - X_1)[1 - \alpha X_1 + 2\alpha X_1^2]$ (not shown). In a similar manner to above, it can be shown that turning points⁶ (X_1^\pm, Y_1^\pm) are given by

$$(X_1^\pm, Y_1^\pm) = \left(\frac{1}{2} \pm \frac{1}{6\alpha} \sqrt{3\alpha(\alpha - 2)}, \frac{1}{2\alpha} \pm \frac{1}{18\alpha^2} \sqrt{3\alpha(\alpha - 2)^3} \right), \quad (53)$$

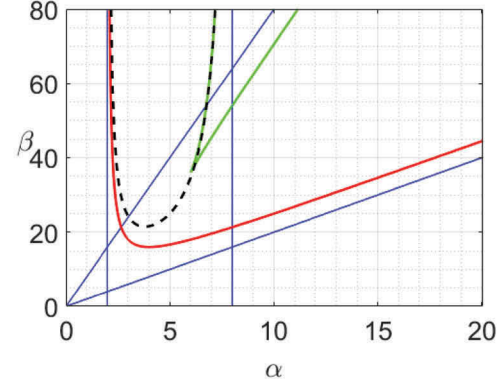
which exist whenever $\alpha > 2$. When $\alpha = 2$, the two nullclines (18), (19), have a cubic tangency at the central equilibrium $(X_1, Y_1) = (X_1^c, Y_1^c) = (X_1^+, Y_1^+) = (X_1^-, Y_1^-) = (\frac{1}{2}, \frac{1}{2\alpha})$. It can be shown that the middle branch of nullcline (19) exists wholly within the permitted phase plane region when $\alpha \in [2, 8]$.

Our aim is to find a curve $\Gamma_v(\alpha, \beta) = 0$ in the (α, β) plane that separates regions where three integrated equilibria are possible from regions where two integrated equilibria are possible. Points on this curve must satisfy:

⁶We retain the same notation for these turning points. No confusion should arise.



(a) $\Gamma_u(\alpha, \beta) = 0$ (equation (52), shown by black dashed line).



(b) $\Gamma_v(\alpha, \beta) = 0$ (equation (56), shown by black dashed line).

Figure 7. Limiting the X_1 -population: $\beta = \beta_c$ (Equation (23), shown in red); $\beta = \beta_{\pm}$ (Equation (31), shown in green), together with the lines $\alpha = 2$, $\alpha = 8$ and $\beta = 2\alpha$, $\beta = 8\alpha$. The points $A = (6, 30)$ and $B = (7, 49)$ correspond to the 2 examples discussed in the main text.

$$Y_1^{\pm} \equiv \frac{1}{2} \pm \frac{1}{18\alpha^2} \sqrt{3\alpha(\alpha - 2)^3} = v, \quad (54)$$

$$X_1^{\pm} \equiv \frac{1}{2} \pm \frac{1}{6\alpha} \sqrt{3\alpha(\alpha - 2)} = (1 - \alpha v)(1 - \beta v + 2\alpha\beta v^2). \quad (55)$$

Equation (54) is the statement that the line $Y_1 = v$ intersects both horizontal tangents of nullcline (18). Equation (55) is the statement that points (X_1^{\pm}, v) lie on nullcline (18).

It can be shown that

$$\Gamma_v(\alpha, \beta) \equiv \beta - \frac{54\alpha^2}{(8 - \alpha)(\alpha - 2)(\alpha + 1)}. \quad (56)$$

The curve $\Gamma_v(\alpha, \beta) = 0$ is shown in Figure 7b. It is asymptotic to both the lines $\alpha = 2, 8$. The effect of restricting both the X_1 - and Y_1 -populations can be seen by combining both plots in Figure 7 (not shown).

Both $\Gamma_{u,v}(\alpha, \beta) = 0$ have a minimum at the same value of β . The minimum of Γ_u occurs at the point $(\alpha_u, \beta) \approx (3.798, 21.488)$, where nullcline (15) passes through both the maximum and minimum of nullcline (14). Similarly, the minimum of Γ_v occurs at the point $(\alpha_v, \beta) \approx (5.658, 21.488)$, where nullcline (14) passes through both the maximum and minimum of nullcline (15).

So far in this section, we have only considered the existence of new equilibria when a population is limited. Let us now consider the stability of these new solutions. When the X_1 -population is restricted to $X_1 = u$, the dynamics on this line is governed by the second equation in each of (42) and (43):

$$a_1 \frac{dY_1}{dt} = L(u, Y_1) = (1 - \alpha Y_1)[1 - \beta Y_1 + 2\alpha\beta Y_1^2] - u. \quad (57)$$

The equilibrium $Y_1 = Y_1^u$ of (57) is the solution of (47). There are either one or three real values of Y_1^u , depending on whether the line $X_1 = u$ crosses the nullcline once or three times. Stability is governed by the eigenvalue

$$\lambda_u = -(\alpha + \beta) + 6\alpha\beta Y_1^u - 6\alpha^2\beta(Y_1^u)^2.$$

Analytical progress can be made in finding λ_u , but in general it has to be evaluated numerically. System (57) can never undergo a Hopf bifurcation to a periodic solution since it is only one-dimensional. Similar conclusions apply when the Y_1 -population is restricted to $Y_1 = v$. The dynamics on this line are governed by the first equation in each of (42) and (43):

$$\frac{dX_1}{dt} = K(X_1, v) = (1 - X_1)[1 - \alpha X_1 + 2\alpha X_1^2] - \alpha v, \quad (58)$$

and the stability of the equilibrium $X_1 = X_1^v$ is governed by the eigenvalue

$$\lambda_v - (1 + \alpha) + 6\alpha X_1^v - 6\alpha(X_1^v)^2,$$

which can be evaluated numerically.

We demonstrate the effects of restricting the X_1 -population in two different areas of (α, β) parameter space. First we take $(\alpha, \beta) = (6, 30)$, corresponding to point *A* in Figure 7a, so we are in the light shaded region of Figure 3. When $u = 1$, shown in Figure 8a, we have no restriction on population. We have 5 equilibria: two stable segregated equilibria with their basins of attraction, plus three unstable integrated equilibria (a central unstable node, flanked by two saddles). When $u = 0.8$, we see in Figure 8b that the segregated equilibrium at $(X_1, Y_1) = (1, 0)$ is no longer accessible, being replaced by a (slightly) integrated stable equilibrium. The three unstable integrated equilibria still survive. A further decrease to $u = 0.71$ produces two extra equilibria (Figure 8c). One of these is a stable highly integrated equilibrium, but it has a small basin of attraction, shown in white to the left of the line $X_1 = 0.71$. This equilibrium only exists for $u \in [X_1^a, X_1^+]$. When $u = 0.6$ (Figure 8d), we see that we have lost two equilibria, leaving us with just two equilibria on the line $X_1 = 0.6$, with only the lower one being stable. Subsequent reduction to $u = 0.4$ leads to a loss of a further two equilibria (Figure 8e). Finally when $u = 0.29$, we lose yet another pair of equilibria, leaving only the stable equilibrium at $(X_1, Y_1) = (0, \frac{1}{\alpha})$.

In our second case, we take $(\alpha, \beta) = (7, 49)$, corresponding to point *B* in Figure 7a, so we are in the dark shaded region of Figure 3. Now we have 9 equilibria, two of which correspond to stable integration. The effect of restricting the X_1 -population is shown in Figure 9, for $u = 1, 0.89, 0.75, 0.25, 0.11, 0.09$.

Hence it can be seen that in the two neighborhood case, restriction of population does not always lead to new integrated equilibria, and those that are produced may only have small basins of attraction. Of possible greater concern is that population restriction can also eliminate integration.

4. Nonlinear tolerance schedules

In this section, we consider other ways in which the linear tolerance schedule can be modified to produce integrated populations. We illustrate phenomena that can occur when the tolerance schedules are nonlinear, using the original Equations (1) in their unscaled form, without restricting the population. We use the exponential and polynomial tolerance schedules, *RE* and *RQ* respectively, introduced in our single neighborhood model (Haw & Hogan, 2018). Both of these imitate Schelling's own sketches of nonlinear tolerance schedules (Schelling, 1971). The characteristic shape is also derived in (Clark, 1991) for the majority? population. We to study these 2 different functional forms in order to explore the potential for analytic results, and to illustrate the qualitative differences that can arise from between candidates for nonlinear tolerance schedules.

We focus on the case $a = 2, b = 10, k = 1$, that is $(\alpha, \beta) = (2, 20)$. This is the simplest case when the tolerance schedules are linear, corresponding to dynamics in the white region of Figure 3, where we have two stable segregated equilibria and one unstable integrated equilibria. These values of parameters a, b and k in our examples are typical of those introduced by Schelling himself, and are

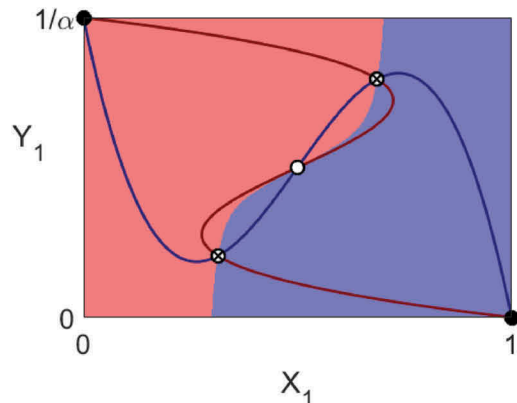
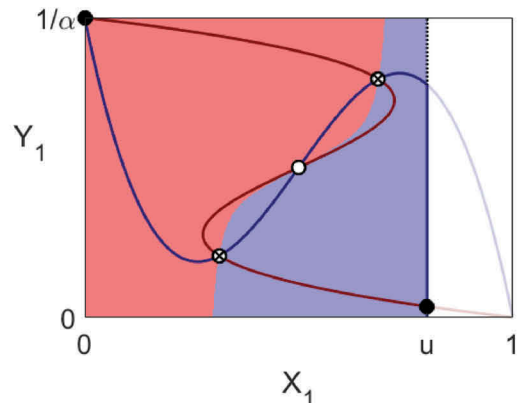
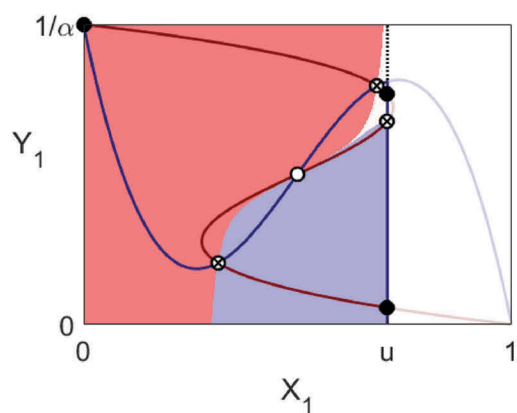
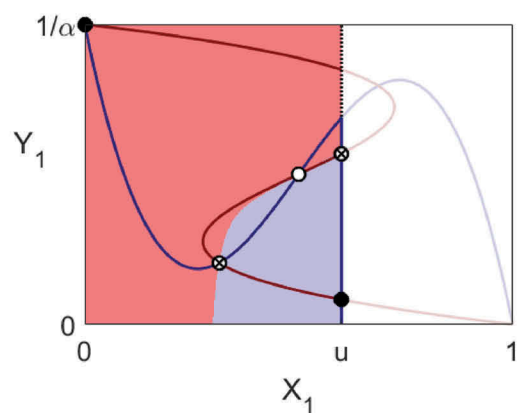
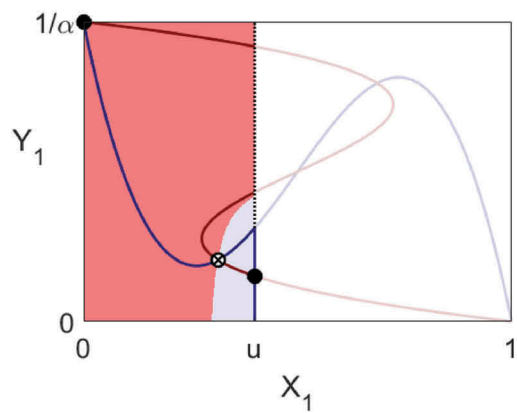
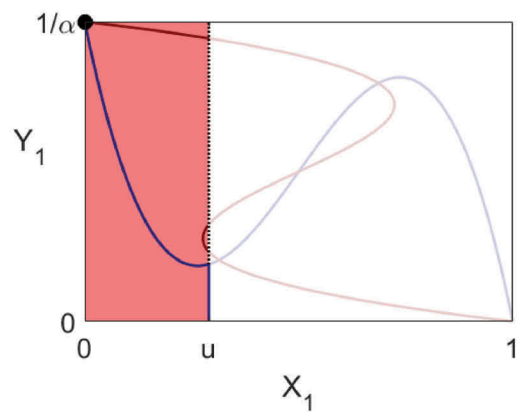
(a) $u = 1$ (b) $u = 0.8$ (c) $u = 0.71$ (d) $u = 0.6$ (e) $u = 0.4$ (f) $u = 0.29$

Figure 8. Limiting the X_1 population: $(\alpha, \beta) = (6, 30)$. Stable equilibria are denoted by \bullet , unstable nodes by \circ and saddle points by \otimes .

chosen in order to best illustrate the qualitatively interesting dynamics that can emerge from our candidate nonlinear tolerance schedules.

In our first example, let us replace the linear X_1 -population tolerance schedule (2) with an exponential tolerance schedule (Haw & Hogan, 2018), of the form

$$R_{X_1}(X_1) = RE_{X_1}^4(X_1) \equiv \frac{2}{1 - e^{-4}} [e^{-4X_1} - e^{-4}], \quad (59)$$

where $RE_{X_1}^4(0) = 2$, $RE_{X_1}^4(1) = 0$. The Y_1 -population has the linear tolerance schedule $R_{Y_1}(Y_1) \equiv 10(1 - Y_1)$. The results shown in Figure 10a are similar to the linear case.

Keeping $R_{X_1}(X_1) = RE_{X_1}^4(X_1)$, we now replace the linear tolerance schedule of the Y_1 -population with an exponential tolerance schedule of the form

$$R_{Y_1}(Y_1) = RE_{Y_1}^4(Y_1) \equiv \frac{10}{1 - e^{-4}} [e^{-4Y_1} - e^{-4}], \quad (60)$$

where $RE_{Y_1}^4(0) = 10$, $RE_{Y_1}^4(1) = 0$. In this case, the central fixed point – a fully integrated population in both neighborhoods – is now stable, with a large basin of attraction (Figure 10b). However, near the saddle points, a small change in initial conditions can lead to a stable segregated population.

Next, consider polynomial tolerance schedules (Haw & Hogan, 2018), of the form

$$R_{X_1}(X_1) = RQ_{X_1}^p(X_1) \equiv a(1 - X_1)^p \quad (61)$$

$$R_{Y_1}(Y_1) = RQ_{Y_1}^p(Y_1) \equiv b(1 - kY_1)^p, \quad (62)$$

where $p \in \mathbb{Z}^+$ and $a = 2$, $b = 10$, $k = 1$, that is $(\alpha, \beta) = (2, 20)$, as before. When $p = 1$, we have the linear tolerance schedule case. When $p = 2$, the corresponding nullcline is a straight line in (X_1, Y_1) phase space. In Figure 10c, we set $R_{X_1} = RQ_{X_1}^2$, given by (61) and $R_{Y_1}(Y_1) = 10(1 - Y_1)$, that is, $p = 2$ for X_1 and $p = 1$ for Y_1 . The results are similar to both the linear case and to Figure 10a. However when we set we set $R_{X_1} = RQ_{X_1}^2$, and $R_{Y_1} = RQ_{Y_1}^2$, we have an open set of equilibria, given by the line $\alpha Y_1 = 1 - X_1$, shown in Figure 10d. Any desired population mixture can be obtained simply by the correct choice of initial conditions. However it is clear that this outcome is not robust – any small change in p will lead to a different outcome.

Finally, in Figure 10e, we set $R_{X_1} = RQ_{X_1}^3$, and $R_{Y_1}(Y_1) = 10(1 - Y_1)$. The results are similar to both the linear case and to Figures 10a,c. However when we set we set $R_{X_1} = RQ_{X_1}^3$, and $R_{Y_1} = RQ_{Y_1}^3$, the central fixed point is stable and its basin of attraction covers the whole of phase space, shown in Figure 10f.

RQ_X^3 and RQ_Y^3 represent globally less tolerant populations than the equivalent linear cases. We can interpret the stable fixed point in Figure 10f phenomenon as follows: low tolerance constraints mean that both types are trying to leave both neighborhoods simultaneously. The stable equilibrium therefore represents a best case scenario, rather than a state in which all tolerance demands are satisfied.

So overall we can conclude that modification of the linear tolerance schedule of only one population may not be enough to induce integration. Instead, both populations may need to modify their tolerance schedules to become integrated.

5. Discussion

Schelling (Schelling, 2006) states that “[in the BNM] ... an important phenomenon can be that a too-tolerant majority can overwhelm a minority and bring about segregation”. We have that

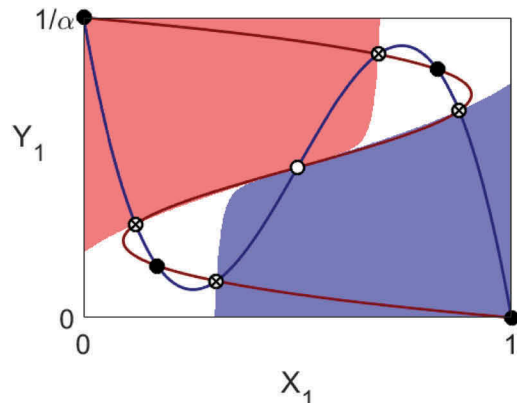
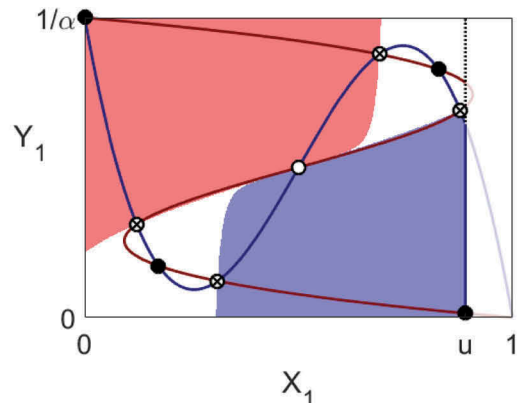
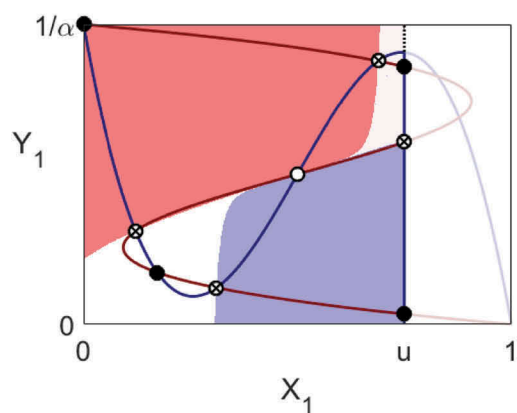
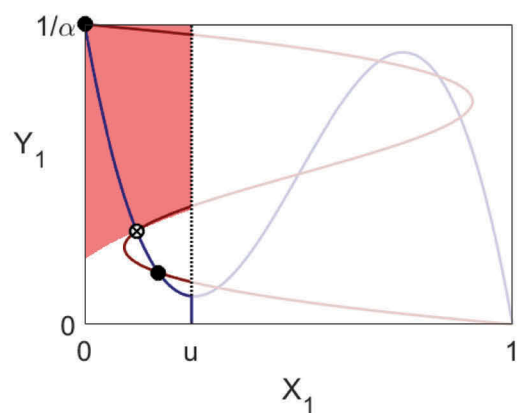
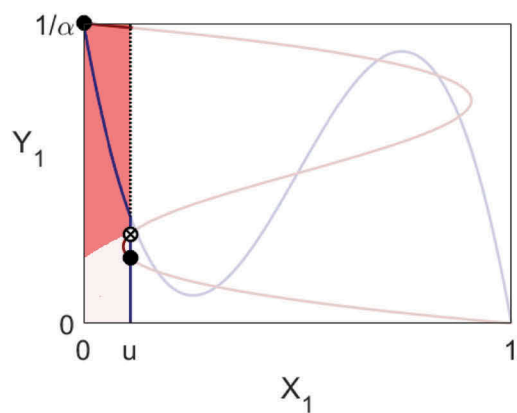
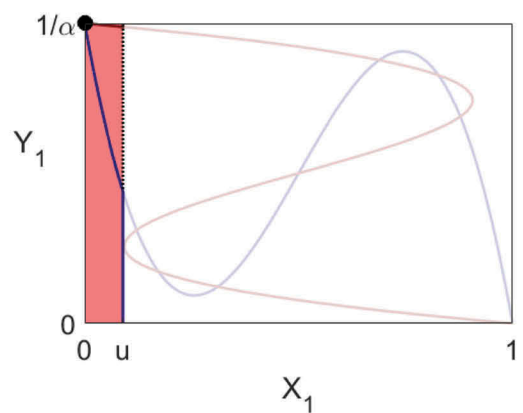
(a) $u = 1$ (b) $u = 0.89$ (c) $u = 0.75$ (d) $u = 0.25$ (e) $u = 0.11$ (f) $u = 0.09$

Figure 9. Limiting the X_1 population: $(\alpha, \beta) = (7, 49)$. Stable equilibria are denoted by \bullet , unstable nodes by \circ and saddle points by \otimes .

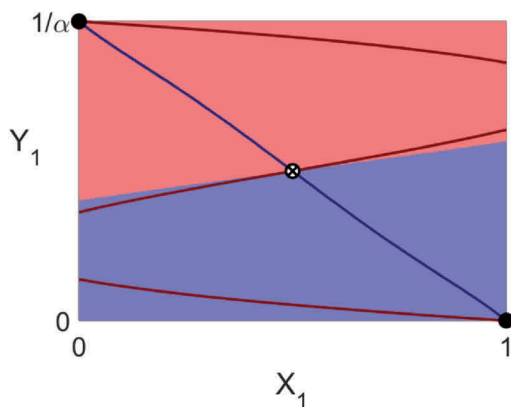
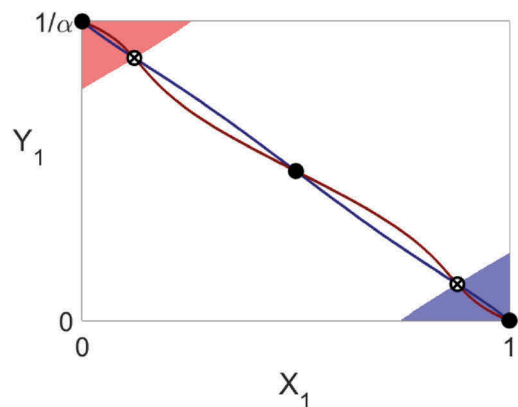
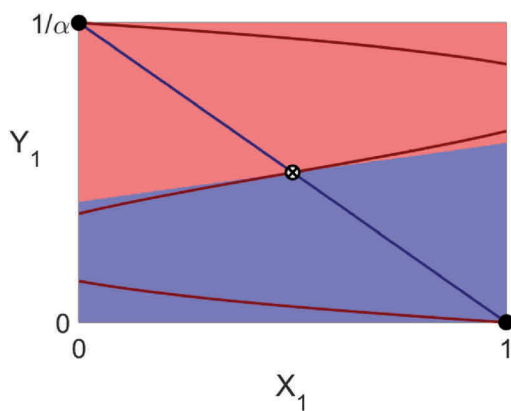
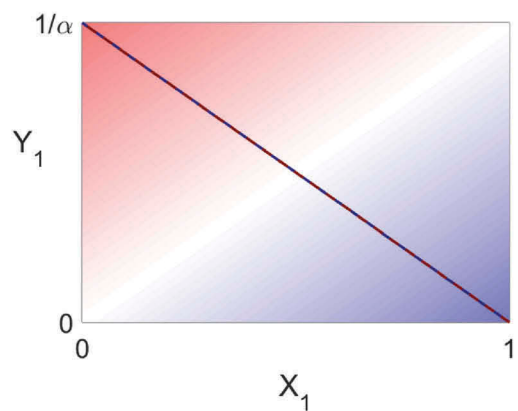
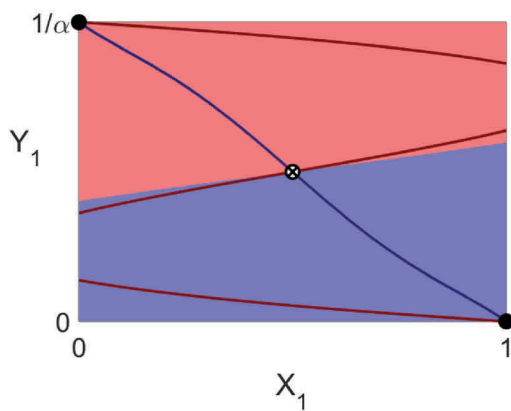
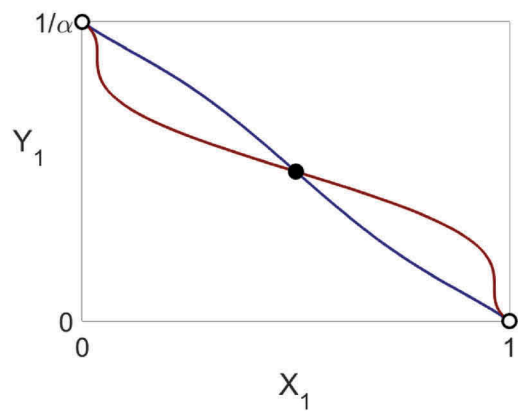
(a) $R_{X_1} = RE_{X_1}^4; R_{Y_1} = 10(1 - Y_1)$.(b) $R_{X_1} = RE_{X_1}^4; R_{Y_1} = RE_{Y_1}^4$.(c) $R_{X_1} = RQ_{X_1}^2; R_{Y_1} = 10(1 - Y_1)$.(d) $R_{X_1} = RQ_{X_1}^2; R_{Y_1} = RQ_{Y_1}^2$.(e) $R_{X_1} = RQ_{X_1}^3; R_{Y_1} = 10(1 - Y_1)$.(f) $R_{X_1} = RQ_{X_1}^3; R_{Y_1} = RQ_{Y_1}^3$.

Figure 10. Nullclines, fixed points and basins of attraction for some candidate nonlinear tolerance schedules. Stable equilibria are denoted by \bullet , unstable nodes by \circ and saddle points by \otimes .

$$\frac{\beta}{b} = a = \frac{\alpha}{k}.$$

So $\beta = \frac{b}{k}\alpha$. Hence lines through the origin of (α, β) parameter space correspond to increasing a , the upper tolerance limit of the majority X -population. We show two of these lines in Figure 7, for $\frac{b}{k} = 2, 8$ corresponding to the case when middle branch of nullcline (19) both exists and lies wholly within the allowed phase space. As we can see, asymptotic to that range is the area of existence of stable integration. Outside that range, even if a is very big, we can not get stable integration, thus quantifying Schelling's (Schelling, 2006) statement.

So far, we have only considered equilibria of our governing Schelling dynamical system (10). Do these equations have periodic solutions? They have been observed in discrete time “two rooms” models of segregation. But these oscillations appear to be neutrally stable and consist of population swings in both rooms. Periodic solutions have also been observed (Gramlich, Plitzko, Rudolf, Drossel, & Gross, 2016; Jansen, 2001) in Lotka-Volterra predator-prey models in two habitats (or patches). But there the dynamics is substantially different.

In our case, we have not found any Hopf bifurcations in our calculations and extensive numerical simulations have not produced any limit cycles. So if they exist, they are most likely unstable (or have a very small basin of attraction). Since (10) is a planar system, Dulac's criterion (Jordan & Smith, 1999) could be used to show that (10) does not have limit cycles. But up to now, we have been unable to find the correct Dulac function. So the existence and stability of periodic solutions to (10) must remain an open question.

We can use our results to consider the effects of variation in parameters α and β . In particular we are interested in what might happen as the minority Y -population grows. Provided the variation is slow enough to be considered quasi-static, we can simply move around parameter space. A key parameter is $\alpha \equiv ak$. If we fix a , the maximum tolerance of the X -population, and then decrease k , the Y -population grows as α decreases. Then for fixed combined tolerance parameter $\beta \equiv ab > 36$ in Figure 3, we see that integration is only a transient phase as we enter and then leave the dark shaded region. So as k decreases, we need to ensure that α stays fixed, and that can only happen if a increases. In other words, when a minority grows, stable integration is only possible if the majority population increases its own tolerance as well. This runs counter to the populist idea that a growing minority should integrate more into the majority to be accepted.

In (Haw & Hogan, 2018), we considered the case where the two populations could live either in one neighborhood or remove themselves to a place “where color does not matter” (Schelling, 1971). Suppose now that this place changes in such a way that color does matter. This could happen for example by the creation or removal of borders or as the result of a change in government. If there is an integrated population in the single neighborhood, will it remain integrated after the change to two neighborhoods?

If we overlay part of Figure 3 with part of Figure 2 of (Haw & Hogan, 2018), we obtain Figure 11. We can now make the following observation: in the light shaded region of Figure 11 with apex P_1 , a single neighborhood can have a stable, integrated population. But, for the two neighborhood case, a stable integrated population is possible only in the dark shaded region with apex P_2 .

We then arrive at the remarkable conclusion that, if the minority population is such that its values of α, β lie in the light shaded region, a re-organization of neighborhoods can lead to the loss of the stable integrated population, without any change in the numbers or attitudes of *either* population. Put another way, some types of minority population in two neighborhoods can only achieve integration by creating one neighborhood and a place where type does not matter, or after a perturbation of the system (tipping) into the basin of attraction of an integrated equilibrium.

The two curves shown in Figure 11 appear similar. In fact, a simple mapping takes one curve into the other. Apex P_2 has coordinates $(\alpha, \beta) = (6, 36)$, whereas at apex P_1 , $(\alpha, \beta) = (3, 9)$. If we set $(\alpha, \beta)_{2-\text{neighbourhood}} = (2\alpha, 4\beta)_{1-\text{neighbourhood}}$ in (30), then we recover Equation (9) of (Haw & Hogan,

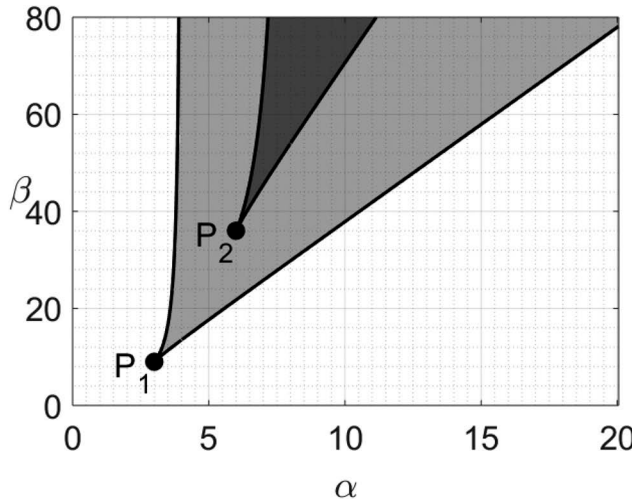


Figure 11. Comparison of integrated population parameters for two-neighborhoods with the single-neighborhood problem (Haw & Hogan, 2018). Curves with apex $P_1 = (3, 9)$ are $\beta = \beta_{\pm}$ from (Haw & Hogan, 2018). Curves with apex $P_2 = (6, 36)$ are $\beta = \beta_{\pm}$ from (31) above.

2018). Both regions in parameter space correspond to values for which cubic discriminants are equal to zero, hence the similarity in shape. The the upper right (or lower left) portion of the 2-neighborhood phase space certainly resembles the single neighborhood model. This plus the similarity of the curves discussed above may lead one to conjecture that each 2-neighborhood system has an equivalent single-neighborhood system with higher tolerance values. It can be shown, however, that the governing dynamical systems can not be mapped (continuously) to one another: 2 systems are fundamentally different to one another.

We can extend the two-neighborhood problem, by introducing an option to be in neither neighborhood (Figure 12). Let X_3 and Y_3 denote the X - and Y -populations present in neither neighborhood. These reservoirs are segregated. Thus $X_3 = 1 - X_1 - X_2$ and $Y_3 = \frac{1}{\alpha} - Y_1 - Y_2$. Neighborhoods 1 and 2 are occupied upon demand as follows. People enter a neighborhood when the tolerance in that neighborhood means that they would stay (and of course people leave a neighborhood when the tolerance there means they should leave). To move between neighborhoods, population members must go through either X_3 or Y_3 (in this version of the problem, there is no direct movement between neighborhoods 1 and 2).

If $f_1(X_i, Y_i) = X_i(X_i R_{X_i}(X_i) - Y_i)$, $i = 1, 2$ and $g_1(X_i, Y_i) = Y_i(Y_i R_{Y_i}(Y_i) - X_i)$, $i = 1, 2$, then

$$\frac{dX_1}{dt} = \begin{cases} f_1(X_1, Y_1) & f_1(X_1, Y_1) \leq 0 \text{ OR } X_3 > 0 \\ \max(0, -f_2) & f_1(X_1, Y_1) > 0 \text{ AND } X_3 = 0 \end{cases} \quad (63)$$

$$\frac{dY_1}{dt} = \begin{cases} g_1(X_1, Y_1) & g_1(X_1, Y_1) \leq 0 \text{ OR } Y_3 > 0 \\ \max(0, -g_2) & g_1(X_1, Y_1) > 0 \text{ AND } Y_3 = 0, \end{cases} \quad (64)$$

which is equivalent to the single-neighborhood case with limiting numbers and $u = X_1 + X_3$, $v = Y_1 + Y_3$. We summarize the dynamics in Table 1.

Figure 13 shows the results of simulating this system. For each (α, β) , we simulate 20 randomly selected initial conditions, and compute the index of dissimilarity \mathcal{D} at equilibrium. The conventional definition of dissimilarity (Massey & Denton, 1988) is $\mathcal{D} := \frac{1}{2} [|X_1 - \alpha Y_1| + |X_2 - \alpha Y_2|] \in [0, 1]$, and corresponds to the proportion of the minority population that would have to relocate in order to yield

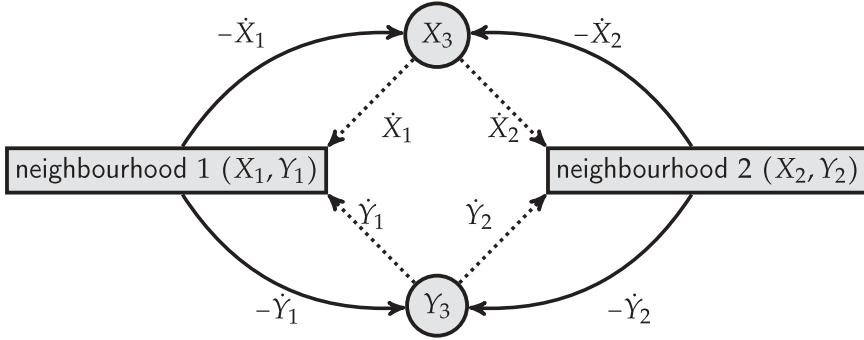


Figure 12. Dynamics of the two neighborhoods problem with reservoirs of population. All arrows represent population flow when the corresponding quantities are positive. Dotted arrows have the additional constraint that $X_3 > 0$ (top part of schematic) or $Y_3 > 0$ (bottom part of schematic).

Table 1. Summary of dynamics for two neighborhoods with population reservoirs, given in (63) and (64). First two columns: $\frac{dx_1}{dt}$. Second two columns: $\frac{dy_1}{dt}$.

$X_3 > 0$	$X_3 = 0$	$Y_3 > 0$	$Y_3 = 0$
$f_1 \leq 0$	f_1	f_1	$g_1 \leq 0$
$f_1 > 0$	f_1	0	$g_1 > 0$
$f_2 \leq 0$	f_2	f_2	$g_2 \leq 0$
$f_2 > 0$	f_2	0	$g_2 > 0$

a uniform distribution of both types across all neighborhoods. One typical criticism of the index of dissimilarity is its sensitivity to neighborhood boundaries. Since boundaries are an inherent property of any BNM, this index is a natural tool to employ in our study.

Our color scale for basins of attraction in cases I-IV uses the modified measure $\bar{\mathcal{D}} := X_1 - \alpha Y_1 \in [-1, 1]$ applied to the corresponding stable equilibrium, in order to distinguish between X_1 - and Y_1 -dominance. A white basin of attraction denotes an even distribution of types in both neighborhoods. In Figure 13, we return to the conventional $\mathcal{D} \in [0, 1]$ as this yields a single measure for the whole system, rather than just one neighborhood.

We repeat this procedure for systems with two neighborhoods without conservation of population, namely two decoupled, single-neighborhood models, as in (Haw & Hogan, 2018). In the former case, the constraint imposed by conservation typically results in stable integrated states. In the latter case, the color scale clearly shows the relative area of basin of attraction of stable segregated states ($\mathcal{D} = 1$), weighted by dissimilarity of the stable integrated states.

6. Conclusion

We have considered Schelling's BNM for the case of two neighborhoods, with and without population reservoirs. In the latter case, we presented the governing dynamical systems in (5) and (6). For the case of identical (X, Y) linear tolerance schedules (case I), we have carried out an extensive analysis, showing both the existence and stability of integration. We have shown that such an outcome requires a small minority, in the presence of a highly tolerant majority. Similar results were obtained when the linear tolerances differ between neighborhoods (cases II, III, IV).

If one or the other population is restricted, by removing the most intolerant individuals, we have shown that new stable population mixtures can be created. But they may only exist in narrow regions of parameter space, with small basins of attraction. In some cases, existing stable integrated populations can even be destroyed by this process. We also considered how different nonlinear tolerance schedules can affect our results.

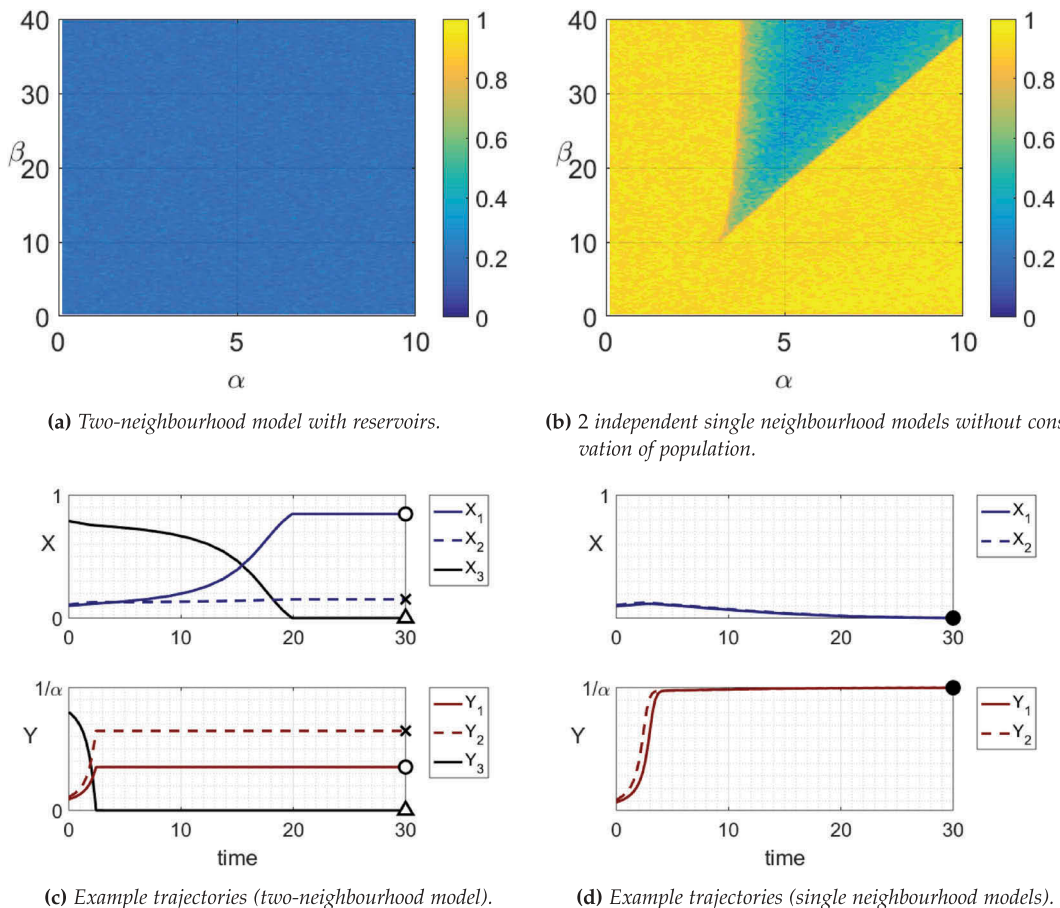


Figure 13. For each (α, β) , we simulated 20 sets of initial conditions for $t = 0$ to $t = 200$, calculated dissimilarity \mathcal{D} for each and plotted the mean \mathcal{D} in parameter space ($\mathcal{D} = 1$ indicates complete segregation, $\mathcal{D} = 0$ indicates an even distribution between neighborhoods). Note that two empty neighborhoods yields $\mathcal{D} = 0$. Results for two neighborhoods with reservoirs are shown in (a), and two independent simulations without conservation of total population are shown in (b). Example trajectories from (a) and (b) are given in (c) and (d) respectively, with $\alpha = 6, \beta = 30, X_1(0) = 0.1, X_2(0) = 0.11, Y_1(0) = 0.09, Y_2(0) = 0.11$.

Similarly the transition from one neighborhood to two neighborhoods (or vice versa) is not necessarily straightforward. A well-integrated single neighborhood can become segregated after such a transition, without any change in the tolerance of either population.

Finally, when considering the case of 2 neighborhoods connected by population reserves, we see that integrated stable states exist for low values of tolerance parameters as a result of competition for finite resources. The notion of trade-off between tolerance demands and external constraints, namely neighborhood structures and finite population reserves, is crucial to understanding the dynamics of segregation. We invite readers from socio-economic disciplines to offer insight into interpretation of our results, and to aid the construction of more complex model variants that better describe the flows of population in real urban areas.

Funding

This work was supported by the Engineering and Physical Sciences Research Council [EP/I013717/1];

ORCID

S. J. Hogan  <http://orcid.org/0000-0001-6012-6527>

References

- Clark, W. A. V. (1991). Residential preferences and neighborhood racial segregation: A test of the Schelling segregation model. *Demography*, 28, 1–19. doi:[10.2307/2061333](https://doi.org/10.2307/2061333)
- Clifton, S. M., Hill, K., Karamchandani, A. J., Autry, E. A., McMahon, P., & Sun, G. (2019). Mathematical model of gender bias and homophily in professional hierarchies. *Chaos*, 29(2), 023135. doi:[10.1063/1.5066450](https://doi.org/10.1063/1.5066450)
- Fossett, M. (2006). Ethnic preferences, social distance dynamics, and residential segregation: Theoretical explorations using simulation analysis. *The Journal of Mathematical Sociology*, 30(3–4), 185–273. doi:[10.1080/00222500500544052](https://doi.org/10.1080/00222500500544052)
- Gramlich, P., Plitzko, S. J., Rudolf, L., Drossel, B., & Gross, T. (2016). The influence of dispersal on a predator-prey system with two habitats. *Journal of Theoretical Biology*, 398, 150–161. doi:[10.1016/j.jtbi.2016.03.015](https://doi.org/10.1016/j.jtbi.2016.03.015)
- Guckenheimer, J., & Holmes, P. (1997). *Nonlinear oscillations, dynamical systems and bifurcations of vector fields*. 5th ed. Berlin, Germany: Springer Verlag.
- Haw, D. J., & Hogan, S. J. (2018). A dynamical systems model of unorganized segregation. *The Journal of Mathematical Sociology*, 42(3), 113–127. doi:[10.1080/0022250X.2018.1427091](https://doi.org/10.1080/0022250X.2018.1427091)
- Hegselmann, R. (2017). Thomas C. Schelling and James M. Sakoda: The intellectual, technical, and social history of a model. *Journal of Artificial Societies and Social Simulation*, 20(3), 15. doi:[10.18564/jasss.3511](https://doi.org/10.18564/jasss.3511)
- Jansen, V. A. A. (2001). The dynamics of two diffusively coupled predator-prey populations. *Theoretical Population Biology*, 59(2), 119–131. doi:[10.1006/tpbi.2000.1506](https://doi.org/10.1006/tpbi.2000.1506)
- Jordan, D. W., & Smith, P. (1999). *Nonlinear ordinary differential equations. An Introduction to dynamical systems* (3rd ed.). Oxford, UK: Oxford University Press.
- Massey, D. S., & Denton, N. A. (1988). The dimensions of residential segregation. *Social Forces*, 67(2), 281–315. doi:[10.2307/2579183](https://doi.org/10.2307/2579183)
- Moller, L. C., & Serbin, L. A. (1996). Antecedents of toddler gender segregation: Cognitive consonance, gender-typed toy preferences and behavioral compatibility. *Sex Roles*, 35(7–8), 445–460. doi:[10.1007/BF01544131](https://doi.org/10.1007/BF01544131)
- Pancs, R., & Vriend, N. J. (2007). Schelling's spatial proximity model of segregation revisited. *Journal of Public Economics*, 91(1–2):1–24. doi:[10.1016/j.jpubeco.2006.03.008](https://doi.org/10.1016/j.jpubeco.2006.03.008)
- Schelling, T. C. (1969). Models of segregation. *The American Economic Review*, 59, 488–493.
- Schelling, T. C. (1971). Dynamic models of segregation. *The Journal of Mathematical Sociology*, 1, 143–186. doi:[10.1080/0022250X.1971.9989794](https://doi.org/10.1080/0022250X.1971.9989794)
- Schelling, T. C. (2006). Some fun, thirty-five years ago. In L. Tesfatsion & K. L. Judd (Eds.), *Handbook of computational economics* (chapter 37, Vol. 2, pp. 1640–1644). Amsterdam, The Netherlands: Elsevier B.V.
- Shin, J. K., & Sayama, H. (2014). Theoretical investigation on the Schelling's critical neighborhood demand. *Communications in Nonlinear Science and Numerical Simulation*, 19(5), 1417–1423. doi:[10.1016/j.cnsns.2013.08.038](https://doi.org/10.1016/j.cnsns.2013.08.038)
- Shin, J. K., Sayama, H., & Choi, S. R. (2016). A state equation for the Schelling's segregation model. *Complex & Intelligent Systems*, 2, 35–43. doi:[10.1007/s40747-016-0012-x](https://doi.org/10.1007/s40747-016-0012-x)